



DIRECTIONAL-WAVE MEASUREMENTS WITH NDBC 3-METER DISCUS BUOYS

APRIL 1990

U.S. DEPARTMENT OF COMMERCE
National Oceanic and Atmospheric Administration
National Data Buoy Center
Stennis Space Center, MS 39529-6000



DIRECTIONAL-WAVE MEASUREMENTS WITH NDBC 3-METER DISCUS BUOYS

**NATIONAL DATA BUOY CENTER
APRIL 1990**

**KENNETH E. STEELE
DAVID WEI-CHI WANG
CHUNG-CHU TENG
NORMAN C. LANG**

**U.S. DEPARTMENT OF COMMERCE
Robert A. Mosbacher, Secretary
National Oceanic and Atmospheric Administration
National Weather Service
National Data Buoy Center
Stennis Space Center, MS 39529-6000**



DIRECTIONAL-WAVE
MEASUREMENTS WITH WIND
PISTON LOGS BOYS

NATIONAL DATA BUOY CENTER
APRIL 1981

ROBERT L. STELL
DAVID W. WANG
GUY W. WANG
ROBERT C. LIND

U.S. DEPARTMENT OF COMMERCE
NATIONAL OCEANIC AND ATMOSPHERIC ADMINISTRATION
NATIONAL DATA BUOY CENTER
NATIONAL SYSTEMS DIVISION
NATIONAL DATA BUOY CENTER
NATIONAL DATA BUOY CENTER
NATIONAL DATA BUOY CENTER

TABLE OF CONTENTS

	PAGE
1.0 INTRODUCTION	1
2.0 ONBOARD-BUOY WAVE MEASUREMENT SYSTEM	1
2.1 TIME SERIES PROCESSES	5
2.2 CO- AND QUAD-SPECTRA	5
3.0 SENSOR, HULL-MOORING, AND WATER DEPTH EFFECTS	7
3.1 HEAVE CO-SPECTRA POWER TRANSFER FUNCTION (PTF)	7
3.2 DIRECTIONAL RESPONSE AMPLITUDE OPERATORS	7
3.3 PHASE ANGLES	8
3.4 HULL-MOORING RESPONSE FUNCTIONS	11
4.0 CALCULATION OF DIRECTIONAL SPECTRUM FUNCTIONS (C_{11} , r_1 , α_1 , r_2 , α_2)	12
5.0 QUALITY CONTROLLING NONDIRECTIONAL SPECTRA USING SLOPE CO-SPECTRA	12
6.0 ON-STATION PERFORMANCE	13
7.0 CONCLUDING REMARKS	23
8.0 ACKNOWLEDGEMENTS	23
9.0 REFERENCES	23
APPENDIX A. DISSEMINATION OF ENVIRONMENTAL DATA	29
APPENDIX B. BUOY CONFIGURATION	31
APPENDIX C. PREDEPLOYMENT TESTING AND CALIBRATION	35

FIGURES

Figure 1. 3-Meter DACT DWA Buoy Configuration	2
Figure 2. Station 45005 in Lake Erie	3
Figure 3. Mooring Configuration for Station 45005	4
Figure 4. Outline of Onboard Buoy DWA System	6
Figure 5. Example of C_{11} , C_{11}^S , α_1 , and α_2 Reported from Station 45005 at 0100 UTC on July 21, 1989	14
Figure 6. Time Series of Heave ($H_{1/3}$) - and Slope ($H_{1/3}^S$) - Based Significant Wave Heights at Station 45005	16
Figure 7. Scatter Plot of Mid-Range Hull Bow Azimuth Angle Versus Sensor-Measured Wind Direction for Complete Data Set from Buoy at Station 45005 During June, July, and August 1989	17
Figure 8. Scatter Plot of Mean Pitch Angle Versus Wind Speed for Complete Data Set from Buoy at Station 45005 During June, July, and August 1989	18
Figure 9. Scatter Plot of Mid-Range Hull Bow Azimuth Angle Versus Sensor-Measured Wind Direction for Limited Data Set from Buoy at Station 45005 During June, July, and August 1989	19
Figure 10. Scatter Plot of Mean Pitch Angle Versus Wind Speed for Limited Data Set from Buoy at Station 45005 During June, July, and August 1989	20
Figure 11. Means and Standard Deviations of R^h/q Versus Frequency, for Wind Speeds in Range ($4 \leq U$ (M/Sec) ≤ 5), Limited Data Set	21

Figure 12. Means and Standard Deviations of R^h/q Versus Frequency, for Wind Speeds in Range ($10 \leq U$ (M/Sec) < 12), Limited Data Set	22
Figure 13. Means and Standard Deviations of ϕ^h Versus Frequency, for ($4 \leq U$ (M/Sec) < 5), Limited Data Set	24
Figure 14. Means and Standard Deviations of ϕ^h Versus Frequency for ($10 \leq U$ (M/Sec) < 12), Limited Data Set	25

1.0 INTRODUCTION

Widely accepted techniques have been developed for the estimation of directional wave spectra from the motions of a pitch-roll buoy that follows the water surface heave and slopes [1]. These estimates of directional wave spectra have a variety of uses [2]. Since 1975 the U. S. National Data Buoy Center (NDBC), at the John C. Stennis Space Center (SSC) in Mississippi, has been developing the equipment and procedures for hourly collection of directional wave data using pitch-roll buoys. Activities through 1985 have been documented [3]. Since 1985 the development of a pitch-roll-buoy wave measurement system called the Directional Wave Analyzer (DWA) [4] has been completed. The DWA is used with an onboard-buoy Data Acquisition Control and Telemetry (DACT) payload [5]. The DACT reports meteorological and wave data to shore through either the east or west Geostationary Operational Environmental Satellite (GOES). Some details of the data dissemination systems are given in Appendix A and references [6] and [7].

The DACT DWA system was first used at sea aboard a 10-meter-diameter discus hull in January 1986. It was thereafter tested aboard the NDBC standard 3-meter-diameter hull, complete with meteorological sensors, beginning in January 1987. On this hull, it has produced good data [8] with various mooring arrangements in both deep and shallow water. During 1987-89, refinement of the 3-meter buoy end-to-end system design and operating procedures has been ongoing. Today it provides operational-quality directional wave and meteorological data at a reasonable cost. During 1989, five such NDBC buoys produced on the order of 20 thousand hourly reports. Near-real-time data from these buoys are being and will be used by the National Weather Service (NWS) and other U.S. government agencies. The archived data from these and similar directional buoys will be used for both engineering and scientific [9] purposes during the next few years.

Many published papers relating to pitch-roll buoy directional data provide too few details about the measurement systems. Incomplete information about sensor characteristics, data processing methods, quality control, and calibration procedures lends uncertainty to interpretations of the data. The main purpose of this paper is to provide these details for NDBC 3-meter DACT DWA type buoys.

Figure 1 depicts the buoy configuration. Appendix B and references [10] and [11] provide details of the hull, mooring, power, communications, and meteorological subsystems. These DACT DWA buoys are essentially identical except for their moorings, which vary from station to station. To illustrate the measurement characteristics of these buoys, we have selected one deployed at station 45005 (see Figure 2).

Station 45005 is located at (41°40'05"N, 82°23'03"W) in southwestern Lake Erie, where the water depth is approximately 14.6 meters. The mooring used at station 45005 is shown in Figure 3. This mooring differed somewhat from other shallow water moorings in that a ballast ball was inserted in an attempt to make the vertical force on the bridle equal to that of a deep-water, inverse catenary mooring.

After deployment on May 12, 1989, the directional wave measurement system operated normally until the buoy ceased reporting on October 15, 1989. Failure was due to a bullet from a person unknown. Wind sensors 1 and 2 failed, respectively, on August 16 and October 2, 1989 (wind sensors have been the most fragile of the buoy's sensors). The directional wave measurement system used aboard this and similar 3-meter buoys is described in Section 2.0.

2.0 ONBOARD-BUOY WAVE MEASUREMENT SYSTEM

The directional wave spectrum can be written as the product of the nondirectional frequency spectrum, $C_{11}(f)$, and the spreading function, $D(f,\alpha)$. Thus,

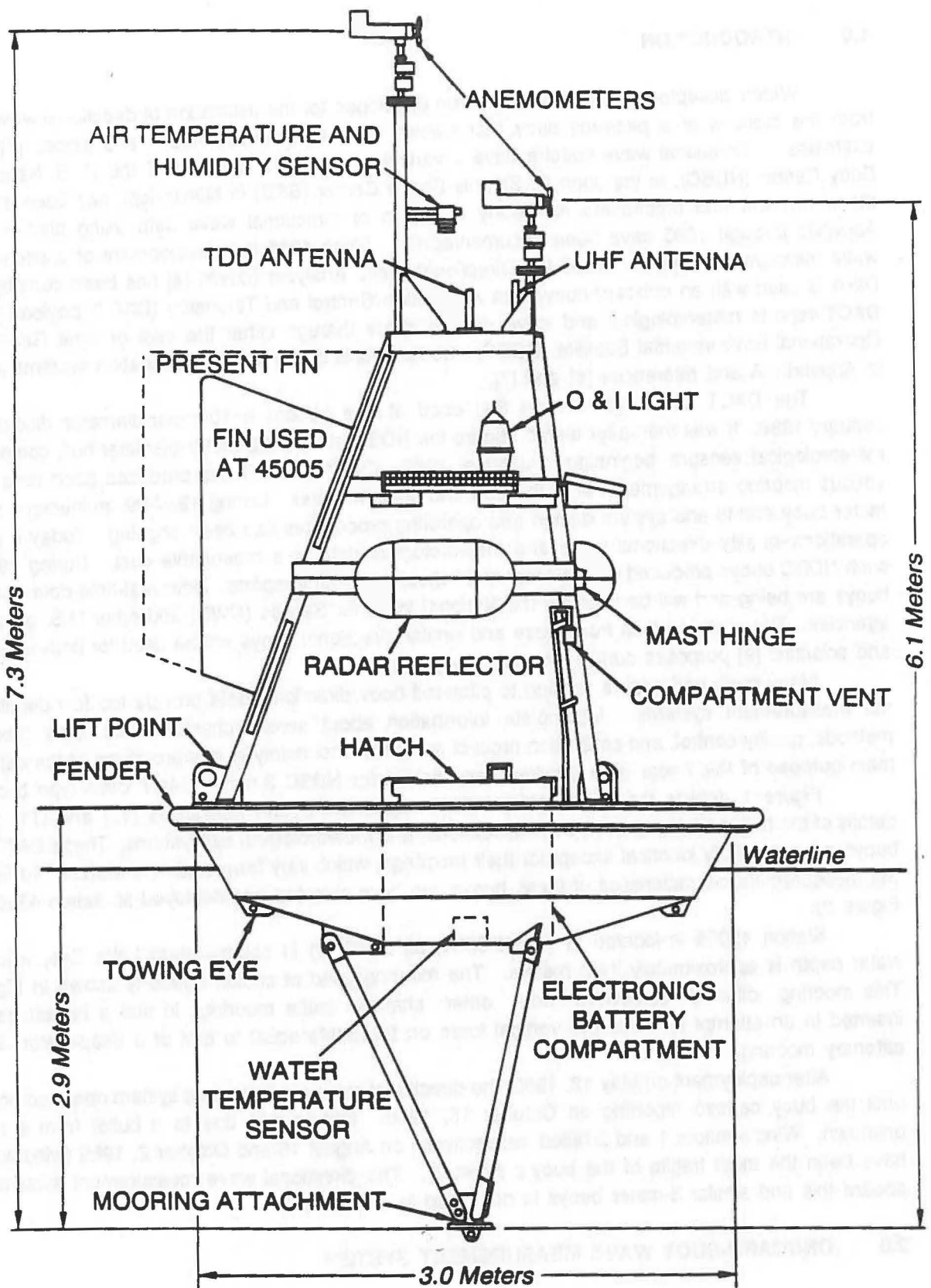


Figure 1. 3-Meter DACT DWA Buoy Configuration

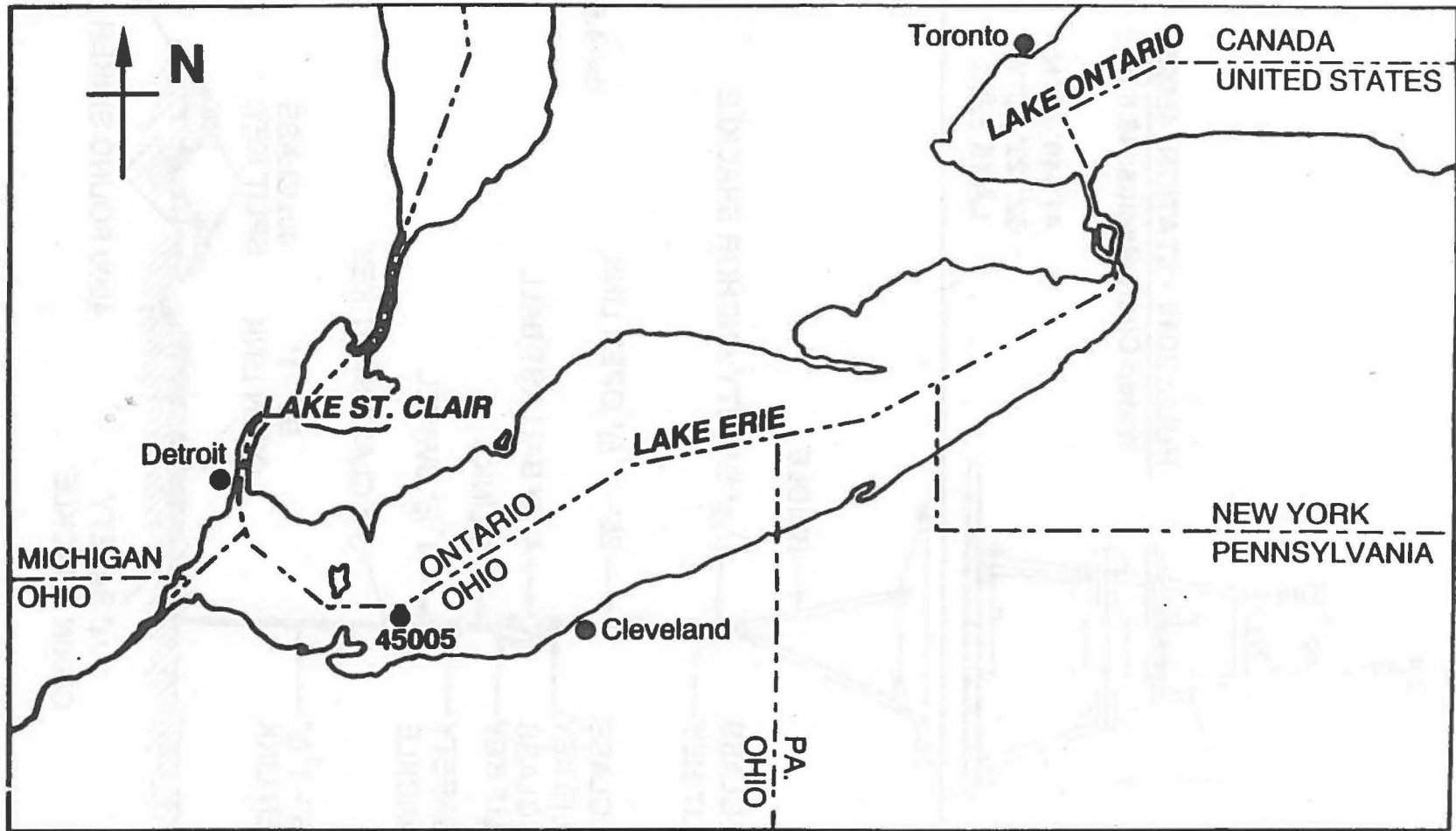


Figure 2. Station 45005 In Lake Erie

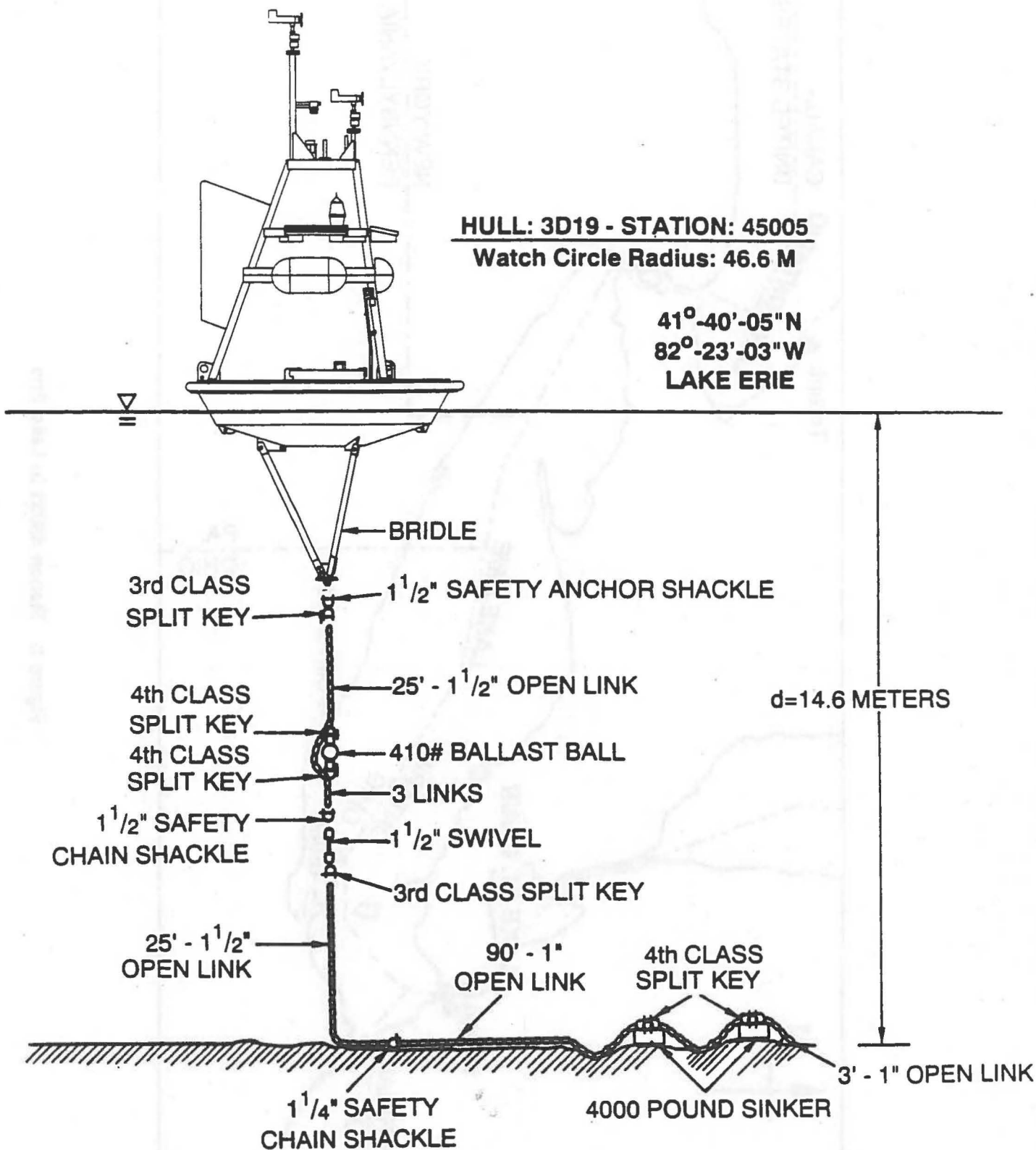


Figure 3. Mooring Configuration for Station 45005

$$S(f,\alpha) = C_{11}(f)D(f,\alpha) \quad (1)$$

in which f is the wave frequency and α is the direction, clockwise relative to north, from which the waves are arriving. The spreading function can be written as a Fourier series,

$$D(f,\alpha) = \{1/2 + \sum_1^{\infty} r_n \cos[n(\alpha - \alpha_n)]\} / \pi \quad (2)$$

Only the terms through $n = 2$ can be estimated from the motions of a pitch-roll buoy. The frequency-dependent parameters C_{11} , r_1 , α_1 , r_2 , and α_2 are computed from buoy heave and slope time series records taken by the DACT DWA system, as explained in the next paragraphs.

2.1 TIME SERIES PROCESSES

Figure 4 outlines the onboard-buoy directional wave hardware and data processing using mathematical symbols defined in [3]. A General Oceanics model 6011-TAMS triaxial magnetometer produces voltages proportional to the bow and starboard magnetic field components inside the hull. Analog voltages proportional to hull heave displacement, sine of hull pitch angle, and sine of hull roll angle are produced by a Datawell HIPPY 40 Mark II sensor. High frequency antialiasing low pass filters that have no effect in the wave-frequencies range connect these 5 sensor outputs to the Magnavox-built DACT DWA electronics. No very-low-pass filters are needed to prevent low-frequency aliasing because the hull is large enough to prevent any sensor signal output above an estimated $f(\text{Hz}) = 0.6$, and the buttoned-up buoy is almost always isolated from radio interference when on station.

As described in more detail in [4], sensor outputs are sampled at 2 Hz for 20 minutes. Counts (12-bit) from the analog-to-digital converter are converted to physical units at 2 Hz, and hull true azimuth angle is immediately calculated. Nine constants stored in the DWA take account of earth local magnetic field components (two constants), hull fixed (two constants) and induced (four constants) magnetism, and local magnetic variation angle ([12],[13]). Based on static tests, computed samples of true azimuth angle are believed to be accurate to at least ± 5 degrees, and are likely accurate to ± 2 degrees. Pitch, roll, and azimuth samples are then used to produce 2-Hz samples of the east-west and north-south slopes of the hull. These and the 2-Hz heave samples from the HIPPY double integrator are numerically low-pass-filtered with a sharp cutoff at about 0.39 Hz. The three filtered 2-Hz records of hull heave and slopes are then subsampled at 1 Hz and stored for further onboard processing.

A number of useful measurements are extracted from the 1-Hz time series records and transmitted to shore. The original azimuth angle at the beginning of the 20-minute record is relayed, as well as means, minimums, and maximums from the heave, pitch, and roll records. Maximum excursions clockwise and counterclockwise from the original azimuth angle, and the maximum tilt (total deviation of the mast away from the earth vertical) are also reported.

2.2 CO- AND QUAD-SPECTRA

The 1-Hz time series records of hull heave (z_1), true east-west slope (z_2), and true north-south slope (z_3) are transformed to six co- and two quad-spectra (C_{11}^m , C_{22}^m , C_{33}^m , C_{23}^m , Q_{12}^m , C_{12}^m , Q_{13}^m , and C_{13}^m , in which C_{ij}^m are the co-spectra, Q_{ij}^m are the quad-spectra, subscripts 1, 2, and 3 represent heave, east-west slope, and north-south slope, respectively, and superscript "m" distinguishes hull-measured values from sea values). Spectra are computed by an FFT applied to windowed 100-second segments that are overlapped by 50 seconds. To keep the GOES message as short as possible, the Q_{23}^m quad-spectrum, which for linear wave theory should be zero, is not produced.

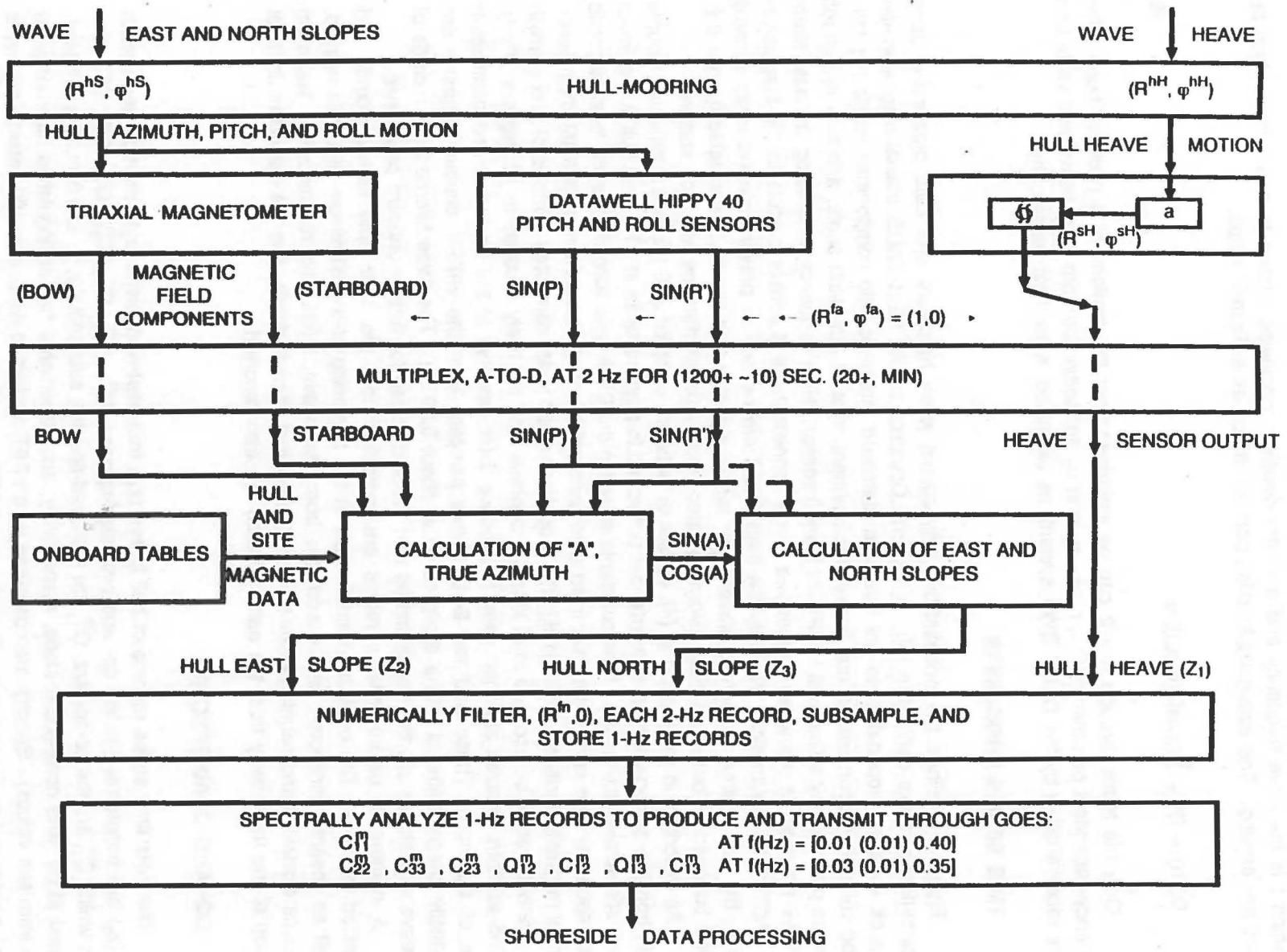


Figure 4. Outline of Onboard Buoy DWA System

Estimates of C_{11}^m are formed by averaging segment values for $f(\text{Hz}) = 0.01, 0.02, 0.03, \dots, 0.39, 0.40$, or, in shorthand, for $f(\text{Hz}) = [0.01(0.01)0.40]$. These C_{11}^m values, and estimates of the other seven spectra formed in the same way but at only $[0.03(0.01)0.35]$ Hz, are produced with approximately 24 degrees of freedom and transmitted to shore. Details are given in [4]. More spectral leakage occurs using short segments [14] than would occur by analyzing the complete record with one FFT. But this leakage is not large enough to affect the usefulness of DWA co- and quad-spectra for operational applications.

To allow accurate reporting of small, in the presence of large, spectral values while minimizing message length, the DWA uses a nonlinear encoding/decoding procedure [15] for transmitting the co- and quad-spectra to shore. The sign of each spectral value in a set of co- or quad-spectrum values is transmitted to shore separately. The associated positive values are then normalized against the largest. The largest is transmitted in floating point form with negligible error. Each of the normalized spectra greater than 0.00001 is logarithmically encoded into an integer count, transmitted to shore, and decoded. This encode/decode process has a mean error of zero and maximum error of ± 0.6 percent, regardless of the magnitude of the normalized spectra.

3.0 SENSOR, HULL-MOORING, AND WATER DEPTH EFFECTS

Assuming that small amplitude wave theory applies, buoy co- and quad-spectra can be converted on shore into sea directional wave data if water depth as well as electrical, numerical, and hull-mooring response amplitude operators (RAO's) and phase lags are taken into account. Two predetermined frequency-dependent calibration data base functions (PTF, the Power Transfer Function, and $\bar{\phi}$, the best available estimate of ϕ , the phase angle) are used to accomplish this. However, a frequency-dependent (RAO, phase angle) combination that is computed from buoy co- and quad-spectra each hour is needed to compensate automatically for heave sensor and hull-mooring responses and for any variations in water depth that may occur. This combination is determined by imposing, as shown in 3.2 and 3.3 below, the requirement that the amplitude and phase relationships between sea heave and sea slope be those of small-amplitude linear wave theory.

3.1 HEAVE CO-SPECTRA POWER TRANSFER FUNCTION (PTF)

Since computer simulation models indicate that hull heave RAO's are insensitive to winds and currents, a PTF that does not change from hour to hour is used to correct C_{11}^m . It is constructed from four frequency-dependent RAO's that are stored in a data base at SSC:

$$\text{PTF} = (R^{hH}R^{sH}R^{fn}R^m)^2 \quad (3)$$

These functions account for the amplitude responses of the hull-mooring (R^{hH}) and displacement sensor (R^{sH}) in heave, the analog antialiasing filtering (none that affect data in the wave-frequency range in the case of the DWA, so $R^{fn} = 1$), and the numerical filtering (R^m) built into the DWA. Values of R^{hH} come from a field test (see Appendix C). Reference [3] describes the sources of the values used for the R^m and R^{sH} .

3.2 DIRECTIONAL RESPONSE AMPLITUDE OPERATORS

According to linear wave theory, sea slope and heave co-spectra are related by

$$k^2 C_{11} = C_{22} + C_{33} \quad (4)$$

in which the wave number k is determined from the linear dispersion relation

$$\omega^2 = gk[\tanh(kd)], \quad (5)$$

where

$$\omega = 2\pi f,$$

g = the gravitational constant, and

d = water depth,

it can be shown (see derivation of equation (51) of [3]) that

$$kR^h/R^{sH} = \sqrt{(C_{22}^m + C_{33}^m)/C_{11}^m} \quad (6)$$

in which (equation (35) of [3])

$$R^h = R^{hS}/R^{hH} \quad (7)$$

where

R^{hS} = the amplitude response of the hull-mooring in pitch and roll at each frequency.

The term on the left side of equation (6) also appears in the expressions for r_1 and r_2 derived from equations (7) - (10), (14), (15), (33), and (34) of [3]. Hull-mooring models available to NDBC are not verified well enough to determine the R^h function needed to compute this combination in advance of deployment for each unique hull-mooring and water-depth combination at each station. Furthermore, for a particular deployed hull-mooring, the combination varies somewhat from hour to hour due to tidal variations and forces on the buoy mooring. These complications make necessary the automatic application of equation (6) each hour in the calculation of r_1 and r_2 . The derivations of equations (52) and (54) of [3] reflect this process.

3.3 PHASE ANGLES

As has been shown by equations (33) through (37) of [3], the hull-mooring-sensor combination shifts the phase of the sea heave/slope quadrature spectra by an angle ϕ , producing the hull-measured co- and quadrature spectra. The angle ϕ is the sum of two angles (equation (36) of [3]),

$$\phi = \phi^{sH} + \phi^h, \quad (8)$$

in which

ϕ^{sH} = HIPPY 40 displacement or acceleration sensor(s)
heave (H) phase lag angle, provided by Datawell,

and (equation (37) of [3])

$$\varphi^h = \varphi^{hH} - \varphi^{hS}, \quad (9)$$

in which

φ^{hH} = hull-mooring (h) heave (H) phase lag angle, and

φ^{hS} = hull-mooring (h) slope (S) phase lag angle.

Like (kR^h/R^{sH}) , φ is considered constant during the 20 minutes of data acquisition. But it varies somewhat as environmental conditions change, leading to the use of an hourly value in equations (40) and (41), used below for the calculation of r_1 and α_1 in equations (38) and (39). A value of φ for each frequency band is computed each hour as follows.

The hull slopes in an earth-fixed frame of reference, which has been rotated clockwise by an angle "a" relative to the true (east-west($z_2(0)$)/north-south($z_3(0)$)) frame of reference, can be written

$$z_2(a) = z_2(0)\cos(a) - z_3(0)\sin(a) \quad (10)$$

$$z_3(a) = z_2(0)\sin(a) + z_3(0)\cos(a). \quad (11)$$

If both sides of (10) and (11) are transformed to the frequency domain, and the heave/slope co- and quad-spectra in the rotated frame of reference are formed, there results

$$C_{12}^m(a) = C_{12}^m(0)\cos(a) - C_{13}^m(0)\sin(a) \quad (12)$$

$$Q_{12}^m(a) = Q_{12}^m(0)\cos(a) - Q_{13}^m(0)\sin(a) \quad (13)$$

$$C_{13}^m(a) = C_{12}^m(0)\sin(a) + C_{13}^m(0)\cos(a) \quad (14)$$

$$Q_{13}^m(a) = Q_{12}^m(0)\sin(a) + Q_{13}^m(0)\cos(a) \quad (15)$$

in which the co- and quad-spectra on the righthand sides are those reported by the buoy.

With the definitions

$$[Q'_{12}(a)]^2 = [Q_{12}^m(a)]^2 + [C_{12}^m(a)]^2 \quad (16)$$

$$[Q'_{13}(a)]^2 = [Q_{13}^m(a)]^2 + [C_{13}^m(a)]^2, \quad (17)$$

it can be shown with equations (12) through (15) that

$$[Q'_{12}(a)]^2 = [\frac{1}{2}][W - Z\cos(2a - b)] \quad (18)$$

$$[Q'_{13}(a)]^2 = [\frac{1}{2}][W + Z\cos(2a - b)] \quad (19)$$

in which

$$W = [Q'_{13}(0)]^2 + [Q'_{12}(0)]^2 \quad (20)$$

$$Z = \sqrt{X^2 + Y^2} \quad (21)$$

$$b = \tan^{-1}(Y, X) \quad (22)$$

NOTE: A comma separating numerator and denominator in the argument of the arc tangent means that the signs of Y and X must be considered separately to place the angle b in the correct quadrant. When a slash (/) is used to separate numerator and denominator, the angle lies in the first or fourth quadrant.

$$X = [Q'_{13}(0)]^2 - [Q'_{12}(0)]^2 \quad (23)$$

$$Y = 2[C_{12}^m(0)C_{13}^m(0) + Q_{12}^m(0)Q_{13}^m(0)]. \quad (24)$$

From equation (19), $Q'_{13}(a)$ will have its largest magnitude(s) at either of two angles, π apart, one of which is

$$a_0 = b/2. \quad (25)$$

Assuming that the best estimate of ϕ each hour for each frequency band can be achieved by using the values of $[C_{13}^m(a), Q_{13}^m(a)]$ corresponding to the earth-fixed frame of reference yielding the largest value of $Q'_{13}(a)$, equations (14) and (15) are used to compute

$$C_{13}^m(a_0) = C_{12}^m(0)\sin(a_0) + C_{13}^m(0)\cos(a_0) \quad (26)$$

$$Q_{13}^m(a_0) = Q_{12}^m(0)\sin(a_0) + Q_{13}^m(0)\cos(a_0). \quad (27)$$

If $[C_{13}^m(a_0), Q_{13}^m(a_0)]$ were used with equation (34) of [3], which is

$$C'_{13}(a_0) = 0 = -Q_{13}^m(a_0)\sin(\phi) + C_{13}^m(a_0)\cos(\phi), \quad (28)$$

to determine ϕ , the result would be

$$\phi = \tan^{-1}[C_{13}^m(a_0)/Q_{13}^m(a_0)] + (0 \text{ or } \pi). \quad (29)$$

To remove this ambiguity of π , the ϕ frame of reference is first rotated by an angle $\bar{\phi}(t)$, which is the best available estimate of ϕ for each frequency band. This estimate is determined from hull-mooring models, or from previously measured data that have been supported by hull-mooring models. The new co- and quadrature spectra are, with (26) and (27), given by

$$y = -Q_{13}^m(a_0)\sin(\bar{\phi}) + C_{13}^m(a_0)\cos(\bar{\phi}) \quad (30)$$

$$x = +Q_{13}^m(a_0)\cos(\bar{\phi}) + C_{13}^m(a_0)\sin(\bar{\phi}). \quad (31)$$

With these values, there is little if any likelihood of selecting the wrong one of the two angles with

$$\varphi = \bar{\varphi} + \tan^{-1}(y/x), \quad (32)$$

whereby φ is forced to lie within ± 90 degrees of $\bar{\varphi}$. For each station with a DWA buoy, a frequency-dependent table of $\bar{\varphi}$ must be maintained because of station-to-station differences (e.g., the buoy at station 45005 has unusually large-magnitude (negative) values for $\bar{\varphi}$, possibly because of the ballast ball in the mooring line). Equation (32) is used each hour to estimate φ for that hour.

3.4 HULL-MOORING RESPONSE FUNCTIONS

Equations (6), (8), and (9) indicate that water depth, hull-mooring, and heave sensor responses determine both the (kR^h/R^{sH}) combination and φ . The manufacturer provides the heave sensor responses (R^{sH}, φ^{sH}) , which can be presumed not to vary significantly from hour to hour. These can be used to determine the combination of water-depth and hull-mooring effects, separate from heave sensor effects. From equation (8), φ^h , which depends only on hull-mooring responses, is given by

$$\varphi^h = \varphi - \varphi^{sH}, \quad (33)$$

which, with equation (32), determines φ^h . To achieve separation of hull-mooring and heave sensor effects for R^h , it is convenient to transform (6). Suppose that a quantity "q" is defined as

$$q = \tanh(kd) = \omega^2/gk. \quad (34)$$

Consistent with small amplitude wave theory, $q = 1$ in deep water; if not in deep water, $(0 < q < 1)$. If k is eliminated between (6) and (34), the result is

$$R^h/q = (gR^{sH}/\omega^2) \sqrt{(C_{22}^m + C_{33}^m)/C_{11}^m}. \quad (35)$$

Since q is usually either 1 or the order of magnitude of 1 for NDBC mooring stations, and R^h approaches 1 at low frequencies for an essentially discus hull, R^h/q can be expected to remain in the vicinity of 1. R^h has been determined [16] both theoretically [17] and from laboratory experiments [18] for essentially discus hulls not affected much by their moorings.

Attempts to use equation (35) to estimate (R^h/q) at every buoy station were partially successful. But the division of apparent noise(s) in the slope co-spectra by small values of ω^2 led to unsatisfactory results at low frequencies. Better estimates of R^h/q than those from (35) were achieved by replacing (C_{22}^m, C_{33}^m) in equation (35) by their noise-corrected values, (N_{22}^m, N_{33}^m) . Relationships between the noise values at [0.04(0.01)0.18] Hz and that at 0.03 Hz were first established for cases where probably no sea energy was present at any of [0.03 (0.01) 0.18]. The energy at 0.03 Hz, which was presumed to be free of ocean energy all (or virtually all) the time, was used in these algorithms every hour to estimate the noise at 0.04 Hz and above, where ocean energy might or might not be present. These noise estimates were deducted from (C_{22}^m, C_{33}^m) to produce (N_{22}^m, N_{33}^m) . Negative values were set to zero. Then from (35),

$$R^h/q = (gR^{sH}/\omega^2) \sqrt{(N_{22}^m + N_{33}^m)/C_{11}^m}. \quad (36)$$

The $(R^h/q, \varphi^h)$ are amplitude and phase functions dependent on water depth and hull-mooring characteristics. At most stations R^h/q , estimated with equation (36) at a particular frequency, will vary on the order of ± 50 percent, and φ^h computed with (32) and (33) will vary on the order of ± 15 degrees. Of course, when computed in this way, environmental variability scatters the estimates. But surely

variability is in part because ocean currents have not been taken into account in equations (35) and (36), and in part because both functions really do vary with changes in mooring line tension arising from surface winds acting on the buoy superstructure. Values of these two functions are computed each hour and saved for hull-mooring performance evaluations.

4.0 CALCULATION OF DIRECTIONAL SPECTRUM FUNCTIONS (C_{11} , r_1 , α_1 , r_2 , α_2)

Nondirectional wave spectra are calculated at $f(\text{Hz}) = [0.03(0.01)0.40]$ with

$$C_{11} = C_{11}^m / \text{PTF}. \quad (37)$$

Significant wave height, $H_{1/3}$, is computed from the area under the C_{11} spectrum, on which peak and average wave period are also based.

The parameters r_1 and mean wave direction, α_1 , are calculated at $f(\text{Hz}) = [0.03(0.01)0.35]$ with

$$r_1 = \sqrt{[(Q'_{12})^2 + (Q'_{13})^2] / [C_{11}^m (C_{22}^m + C_{33}^m)]}, \quad (38)$$

in which the combination (kR^h/R^{sh}) appearing initially in the expression for r_1 has been eliminated through equation (6), and

$$\alpha_1 = (3\pi/2) - \tan^{-1}(Q'_{13}/Q'_{12}), \quad (39)$$

in which

$$Q'_{12} = Q_{12}^m \cos(\varphi) + C_{12}^m \sin(\varphi) \quad (40)$$

$$Q'_{13} = Q_{13}^m \cos(\varphi) + C_{13}^m \sin(\varphi), \quad (41)$$

where φ is computed for each band each hour with equation (32).

The parameters r_2 and principal wave direction, α_2 , are calculated with

$$r_2 = \sqrt{(C_{22}^m - C_{33}^m)^2 + (2C_{23}^m)^2} / (C_{22}^m + C_{33}^m), \quad (42)$$

and, from equation (55) of [3],

$$\alpha_2 = (3\pi/2) - [1/2] \tan^{-1} [2C_{23}^m / (C_{22}^m - C_{33}^m)] + \text{either } 0 \text{ or } \pi, \text{ whichever makes the small angle between } \alpha_1 \text{ and } \alpha_2 \text{ smaller.} \quad (43)$$

5.0 QUALITY CONTROLLING NONDIRECTIONAL SPECTRA USING SLOPE CO-SPECTRA

If equation (36) were first used with a number of hours of data to establish a mean value, (R^h/q) , for a particular hull-mooring, then equation (36) might be solved (with (R^h/q)) each hour for C_{11}^m , which, with (37), would lead to

$$C_{11}^s = C_{11}, \quad (44)$$

in which by definition

$$C_{11}^S = \{(gR^{SH})/[(R^H/q)\omega^2]\}(N_{22}^m + N_{33}^m)/PTF. \quad (45)$$

The righthand side of equation (44) depends on measurements by the heave sensor, whereas the lefthand side depends on measurements by the magnetometer and pitch and roll sensors. Thus, equation (45) might potentially be used to estimate nondirectional spectra without reference to the heave sensor. Such an estimate each hour would be useful in verifying that all elements of the wave measurement system are still functioning normally, and might provide useful estimates of nondirectional spectra for NDBC's operational data users if the heave sensor should fail.

Use of equation (45) led to excellent agreement between C_{11} and C_{11}^S only part of the time. Regressions of $\sqrt{N_{22}^m + N_{33}^m}$ against $\sqrt{C_{11}^m}$ were then performed. Instead of the former intercepting at zero and increasing linearly with the latter, a non-zero intercept could be projected. Furthermore, at large $\sqrt{C_{11}^m}$ values, the $\sqrt{N_{22}^m + N_{33}^m}$ were not quite as large as expected from a linear relationship. These deviations led to a search for an empirical algorithm for C_{11}^S . This effort was reasonably successful, resulting in

$$C_{11}^S = \{(R^{SH}/B)[\tanh^{-1}(\sqrt{N_{22}^m + N_{33}^m}/C_m) - A]\}^2/PTF, \quad (46)$$

in which $C_m = 0.4$, and A and B are frequency-dependent constants that depend on hull-mooring type and water depth. The empirical inverse hyperbolic tangent function arises from the measured slope co-spectra not rising linearly with heave co-spectra at higher energies. This behavior may be due to nonlinear buoy-tilt restraints at the higher wave slopes caused by the buoy bridle [19] (i.e., R^{HS} decreases with energy at large energies). The details of the development of equation (46) are available in an internal NDBC report [20].

Estimates of nondirectional spectra from equation (46) are routinely calculated and compared to C_{11} , as necessary to judge system status. From these slope-based estimates of nondirectional spectra, an estimate of significant wave height is produced for comparison to the value from the heave sensor.

6.0 ON-STATION PERFORMANCE

Every 3-meter DACT DWA buoy is subjected to laboratory and dockside tests to ensure that it is functioning correctly when deployed. Further information on these tests are provided in Appendix C and references [21] and [22]. The ship deploying a 3-meter DACT DWA buoy stands by while technicians observe meteorological and wave conditions, and hull orientations, for 3 hours. Visual data are relayed to SSC via voice-radio where they are compared to buoy reports coming through the GOES. If reports seem reasonable, the ship departs station. Thereafter meteorological and directional wave data are monitored in a variety of ways to ensure quality throughout deployment. Nondirectional spectra are cross checked against wind speed data by use of methods developed for quality controlling wind speed data [23]. NDBC has published evaluations [24] and reviews ([25], [26]) of selected directional wave data.

Strong winds occurred at 45005 between July 19 at 1300 UTC and July 22 at 2100 UTC. Wave height rose to a maximum of 1.37 meters on July 21 at 0100 UTC and then declined. Figure 5 shows (C_{11} , C_{11}^S , α_1 , and α_2) at the time of maximum significant wave height. Also shown is significant wave height in meters, and the estimated wind speed at the 10-meter level based on buoy

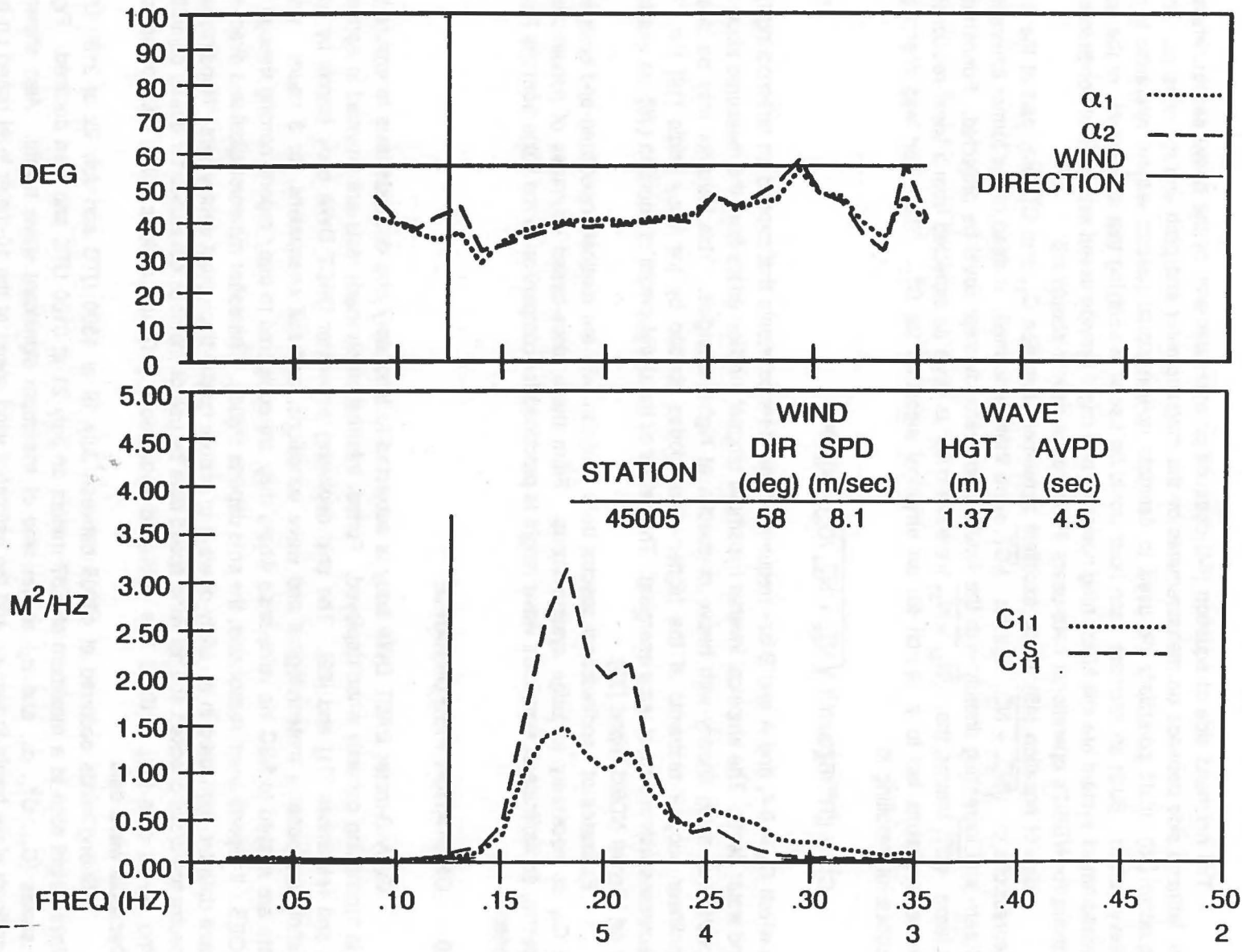


Figure 5. Example of C_{11} , C_{11}^S , α_1 , and α_2 Reported from Station 45005 at 0100 UTC on July 21, 1989

wind speed readings. In support of data quality evaluations, graphs of hourly data such as that of Figure 5 can be produced at SSC for any DACT DWA buoy in a matter of minutes.

Figure 6 compares heave-based ($H_{1/3}$) and slope-based ($H_{1/3}^S$) significant wave heights for the above time period. Although agreement is imperfect, Figure 6 illustrates that slope-based significant wave height can be used to detect gross system failures.

The midpoint of the range of angles through which the bow varies during the 20 minutes of wave data acquisition each hour can be computed from the data sent to shore. Figure 7 is a scatter plot of these mid-range angles versus the corresponding wind sensor directions for all data acquired from station 45005 during June, July, and August 1989 [27]. These data from approximately 2208 hourly reports are called the "original" data set. It can be seen that, for most hours, the bow of the buoy at 45005 is compelled by its fin to face the wind direction to within 20 degrees. The fixed offset of the scattered data away from the 45-degree line suggests either a wind sensor calibration error or asymmetries in the hull superstructure. Another reason for the failure of the points to fall exactly on the 45-degree line in some cases may be that the initial bow azimuth angle is a "snapshot" measured at 25 minutes after the hour, whereas mean wind direction is based on an average over 8 minutes centered on a time 24 minutes later, at minute 49.

With the bow facing the wind, wind drag on the buoy superstructure pitches the bow up, as illustrated by the data in Figure 8, which shows a scatter plot of mean pitch angle versus corresponding wind speed for the original data. Once again, some scatter can be attributed to mean values being calculated over time periods that are separated by 14 minutes.

To illustrate the effect of the minute-to-minute variability in wind speed and direction, a new, limited, data set was formed, taken from the original data set. Those hours for which wind speed did not vary with respect to the values at the preceding and following hours by more than 20%, and for which (simultaneously) the wind direction did not vary with respect to the values at the preceding and following hours by more than 20 degrees, were included in the limited data set. Figures 9 and 10 are repeats of Figures 7 and 8 with the limited data set. The scatter has been noticeably reduced.

It can be seen from Figure 10 that there is a more-or-less quadratic dependence of mean pitch angle on wind speed, as might be expected from the fact that drag force varies as the square of the wind speed. A regression analysis led to the following fit to the data of Figure 10.

$$P = (1.16 \times 10^{-2})U^2 + (8.81 \times 10^{-2})U + 0.29 \quad (47)$$

in which U is in meters/second and P is in degrees.

Although the highest winds used in the production of equation (47) were 13.0 meters/second, it can at least be guessed that in threshold hurricane force winds, a similar buoy may be tilted over to an angle in the neighborhood of 20 degrees. At such a tilt, the directional wave data would have to be regarded with some caution.

The existence of a mean pitch angle for the hull suggests an increased tension in the mooring line in response to an increase in wind speed. Such an increase in tension might alter R^{hs} , which measures the response of hull slope to sea slope. If R^{hh} is not very sensitive to mooring line tension, as simulations would suggest, then R^h might, through R^{hs} , change with increasing wind speed. To investigate this possibility, R^h/q was calculated with equation (36) for all hours and frequencies of the limited data set where $C_{11} \geq 0.01 \text{ m}^2/\text{Hz}$. At each frequency, the data were divided into two categories — cases where the wind fell between 4 and 5 meters/second, and cases where it fell between 10 and 12 meters/second. The means and standard deviations for the two categories were calculated at each frequency and are plotted in Figures 11 and 12. One standard deviation from the mean is indicated by the lines passing through the circles marking the mean values. Since the standard deviations do

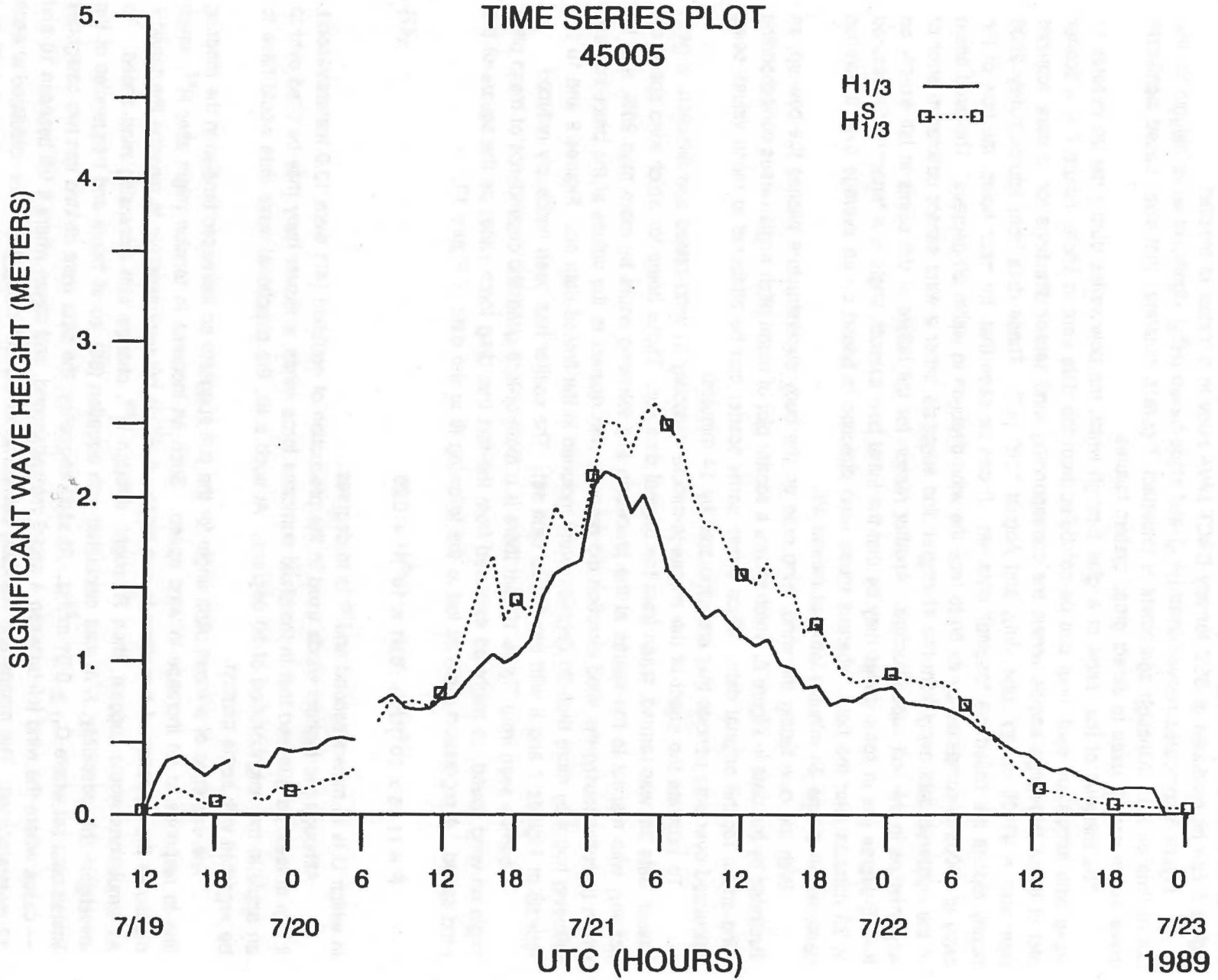


Figure 6. Time Series of Heave ($H_{1/3}$) - and Slope ($H_{1/3}^S$) - Based Significant Wave Heights at Station 45005

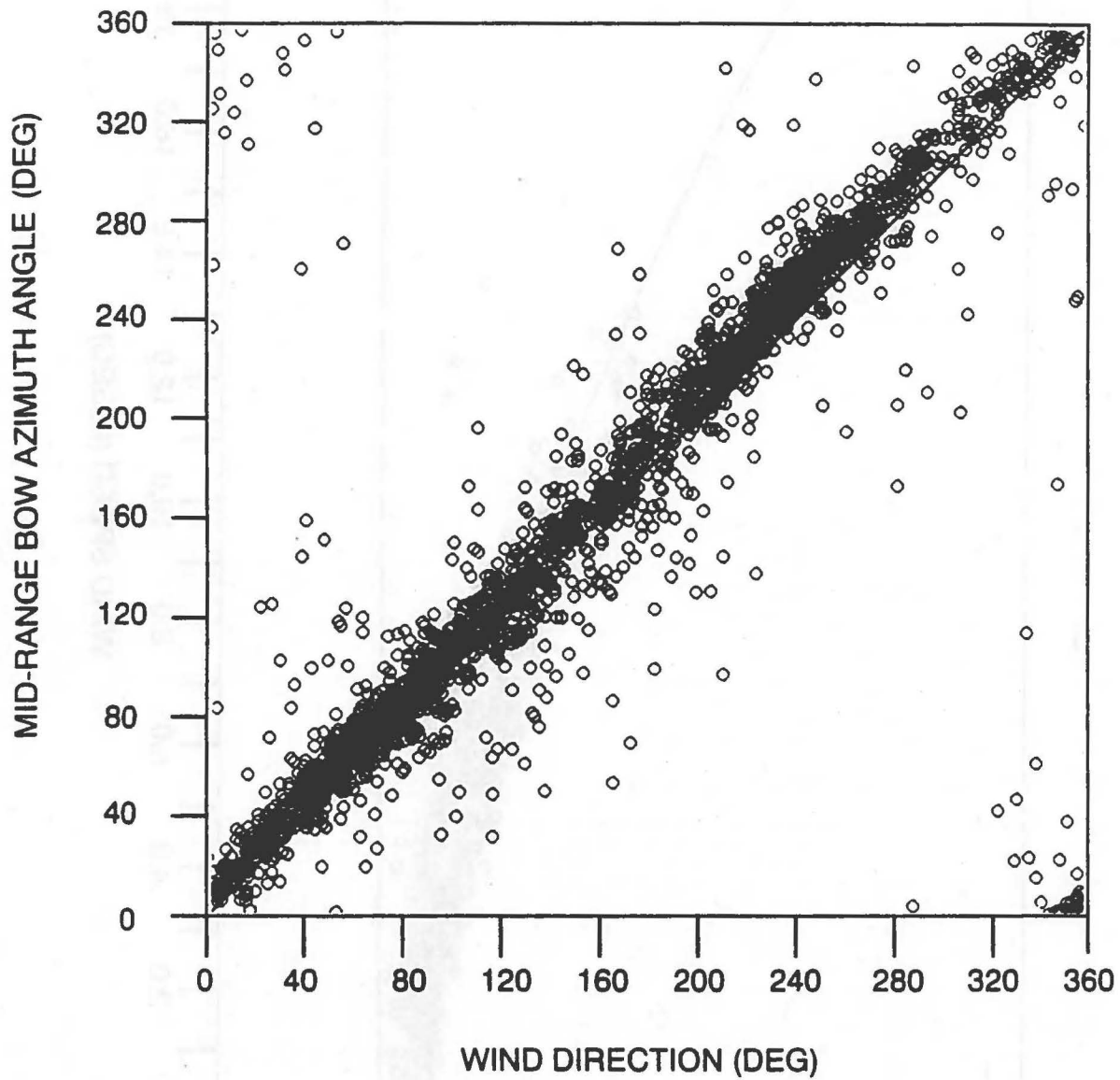


Figure 7. Scatter Plot of Mid-Range Hull Bow Azimuth Angle Versus Sensor-Measured Wind Direction for Complete Data Set from Buoy at Station 45005 During June, July, and August 1989

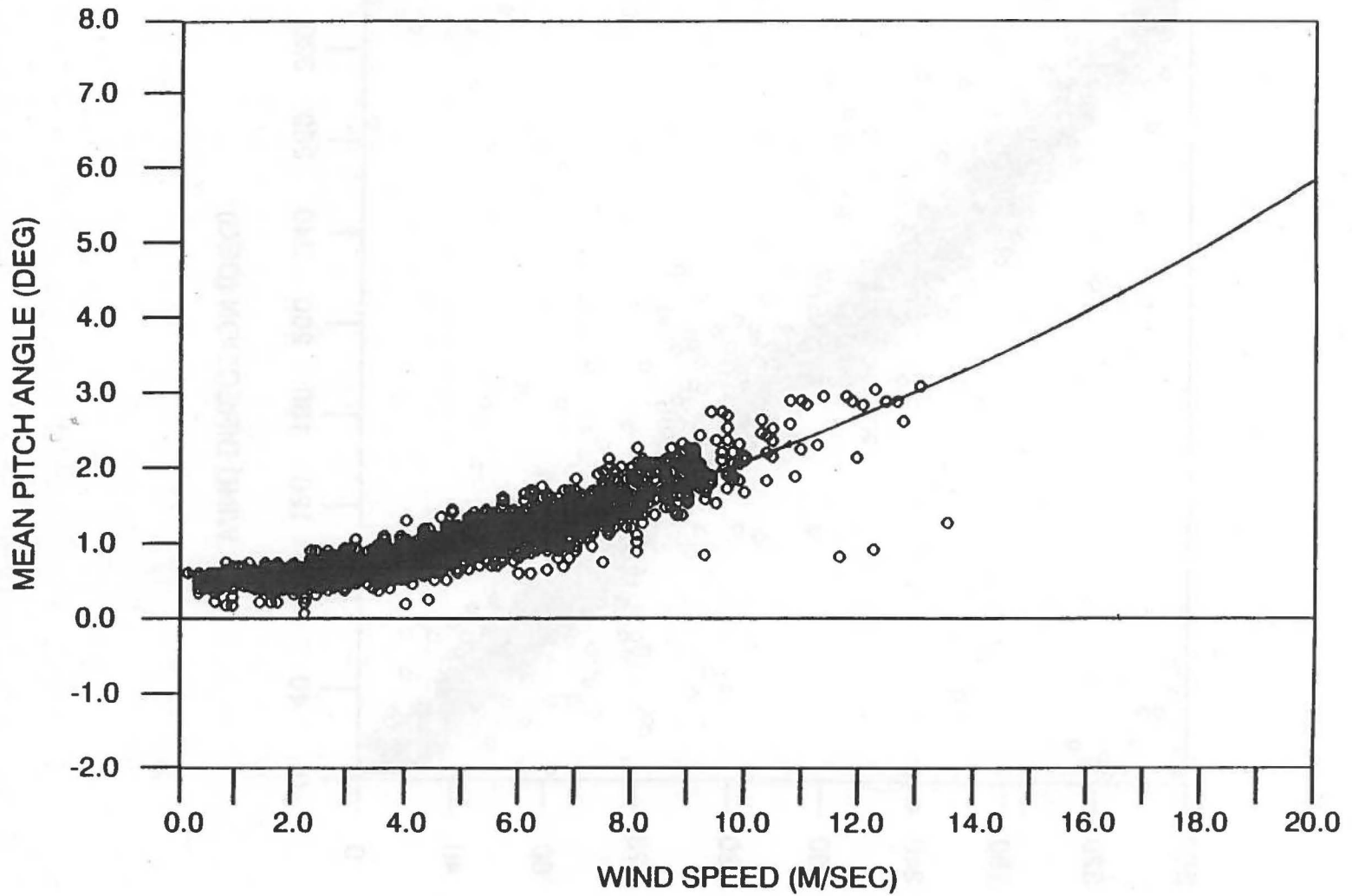


Figure 8. Scatter Plot of Mean Pitch Angle Versus Wind Speed for Complete Data Set from Buoy at Station 45005 During June, July, and August 1989

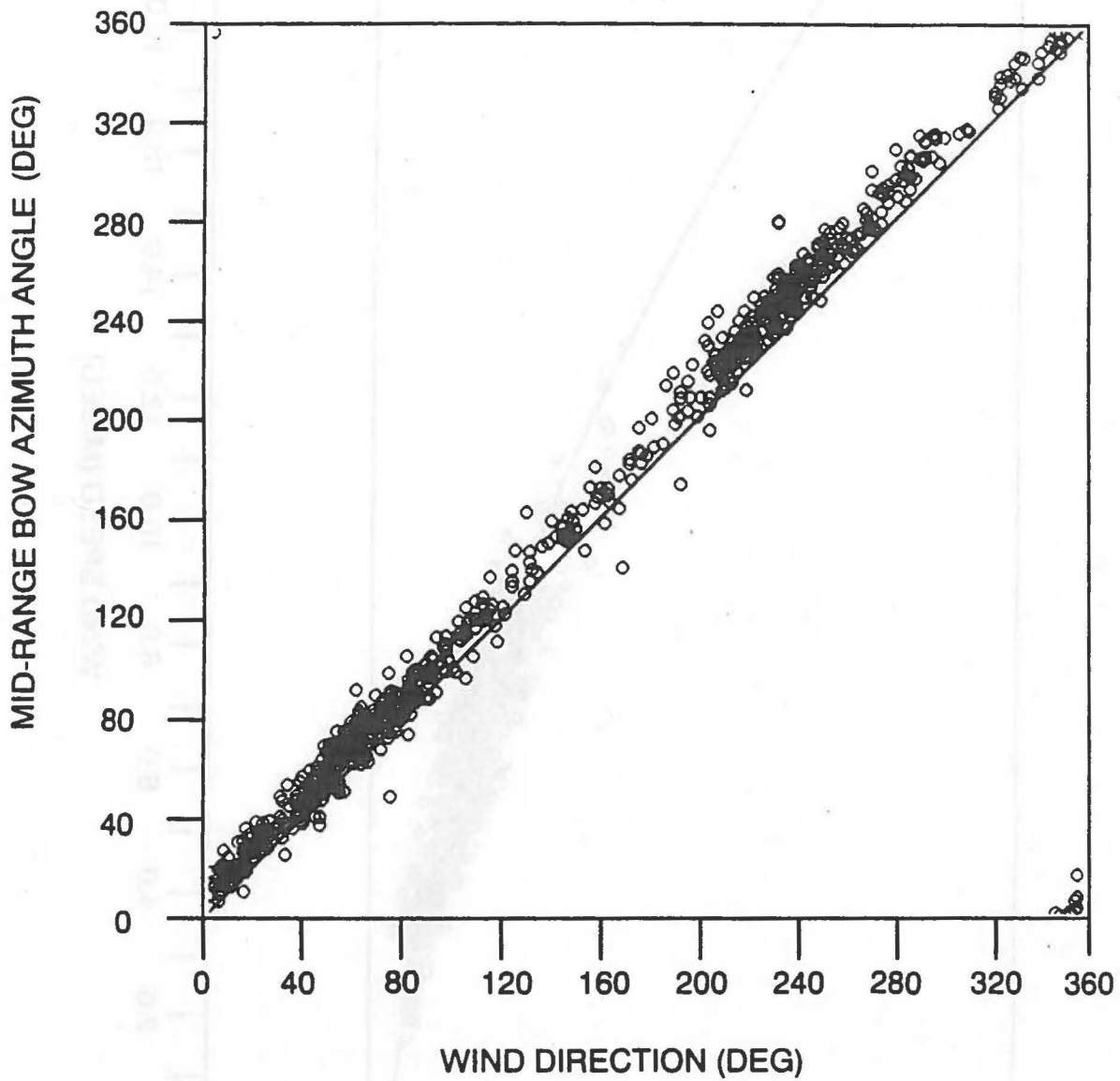


Figure 9. Scatter Plot of Mid-Range Hull Bow Azimuth Angle Versus Sensor-Measured Wind Direction for Limited Data Set from Buoy at Station 45005 During June, July, and August 1989

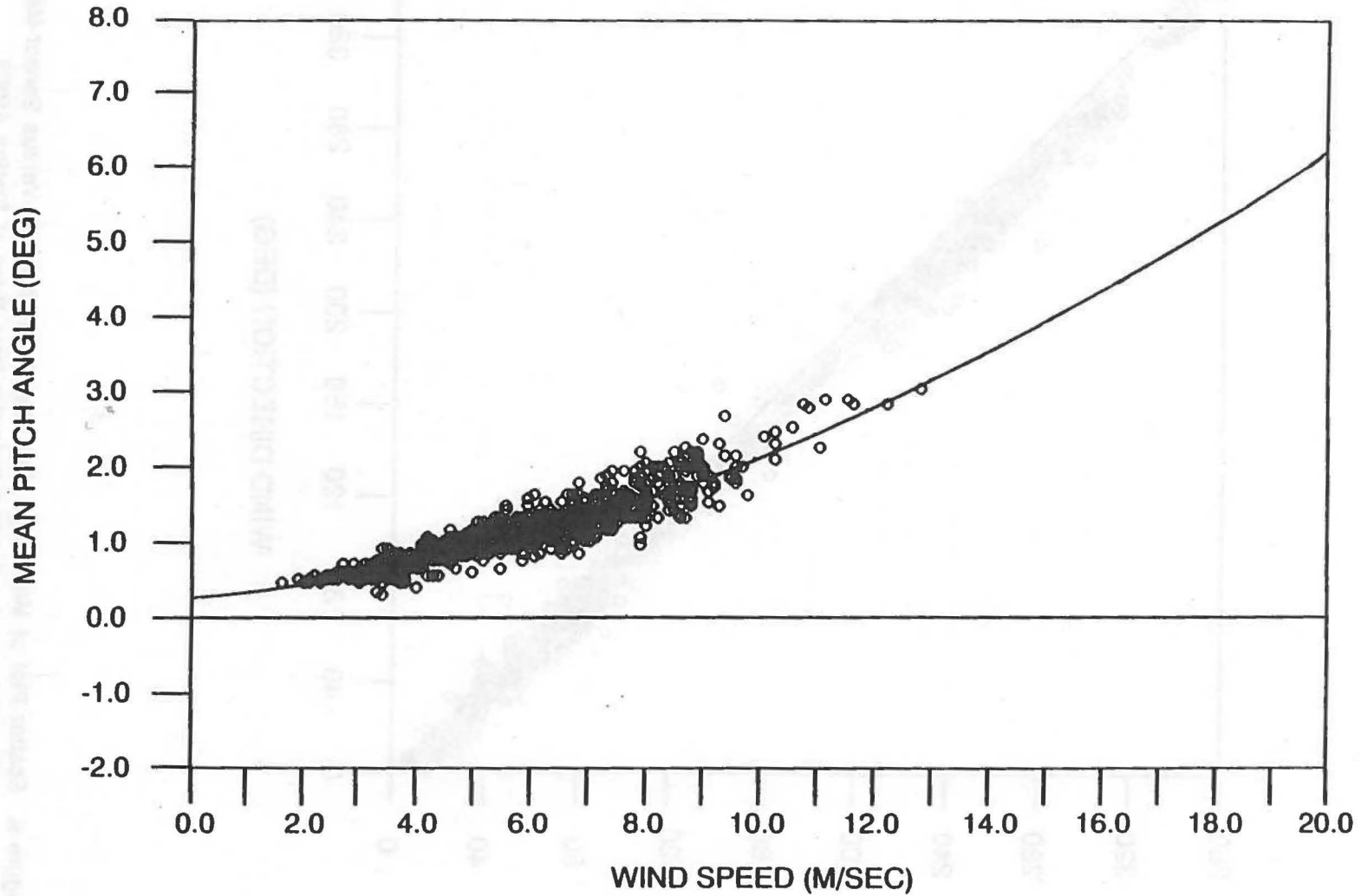


Figure 10. Scatter Plot of Mean Pitch Angle Versus Wind Speed for Limited Data Set from Buoy at Station 45005 During June, July, and August 1989

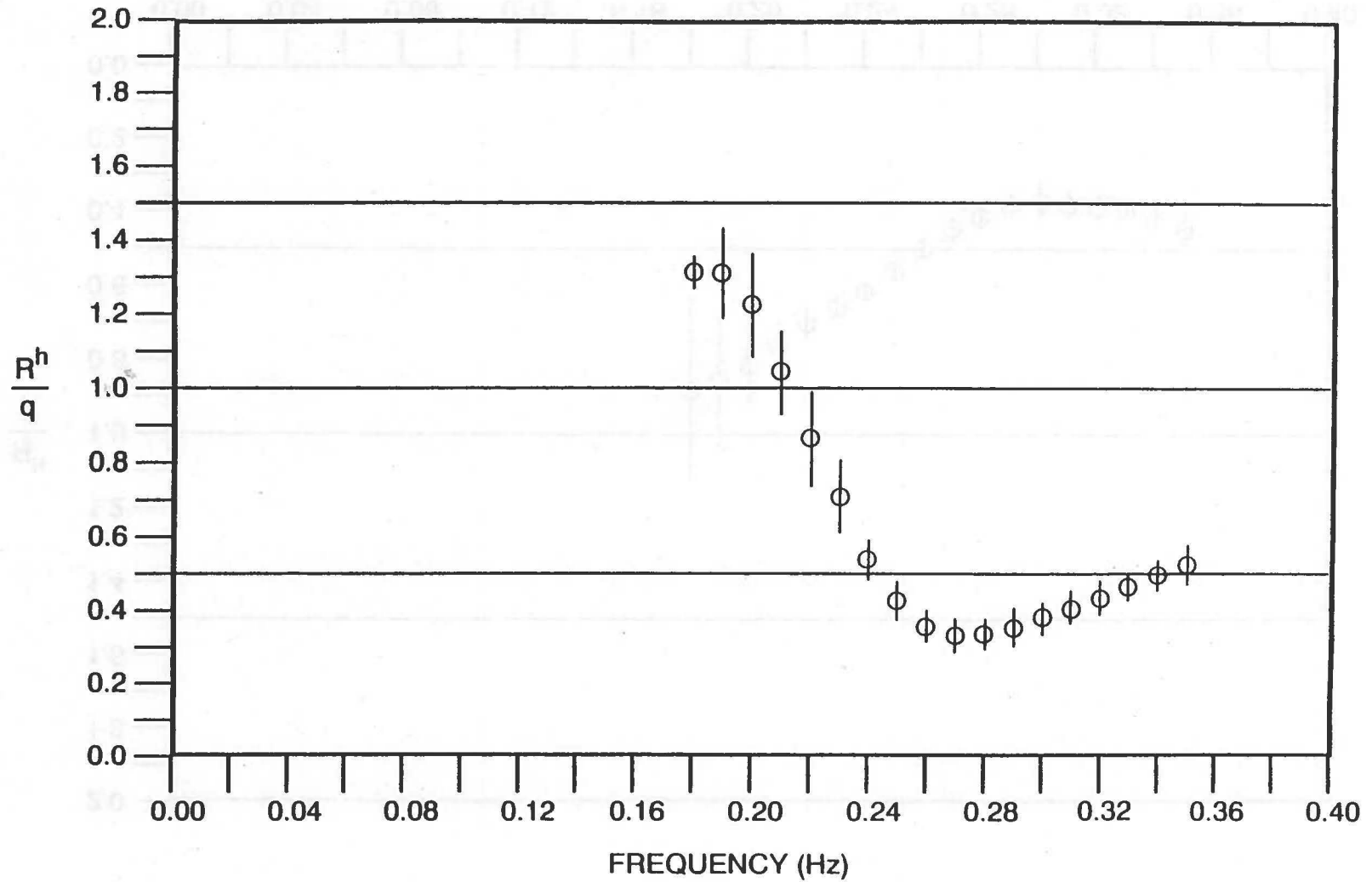


Figure 11. Means and Standard Deviations of R^h/q Versus Frequency, for Wind Speeds In Range ($4 \leq U$ (M/Sec) ≤ 5), Limited Data Set

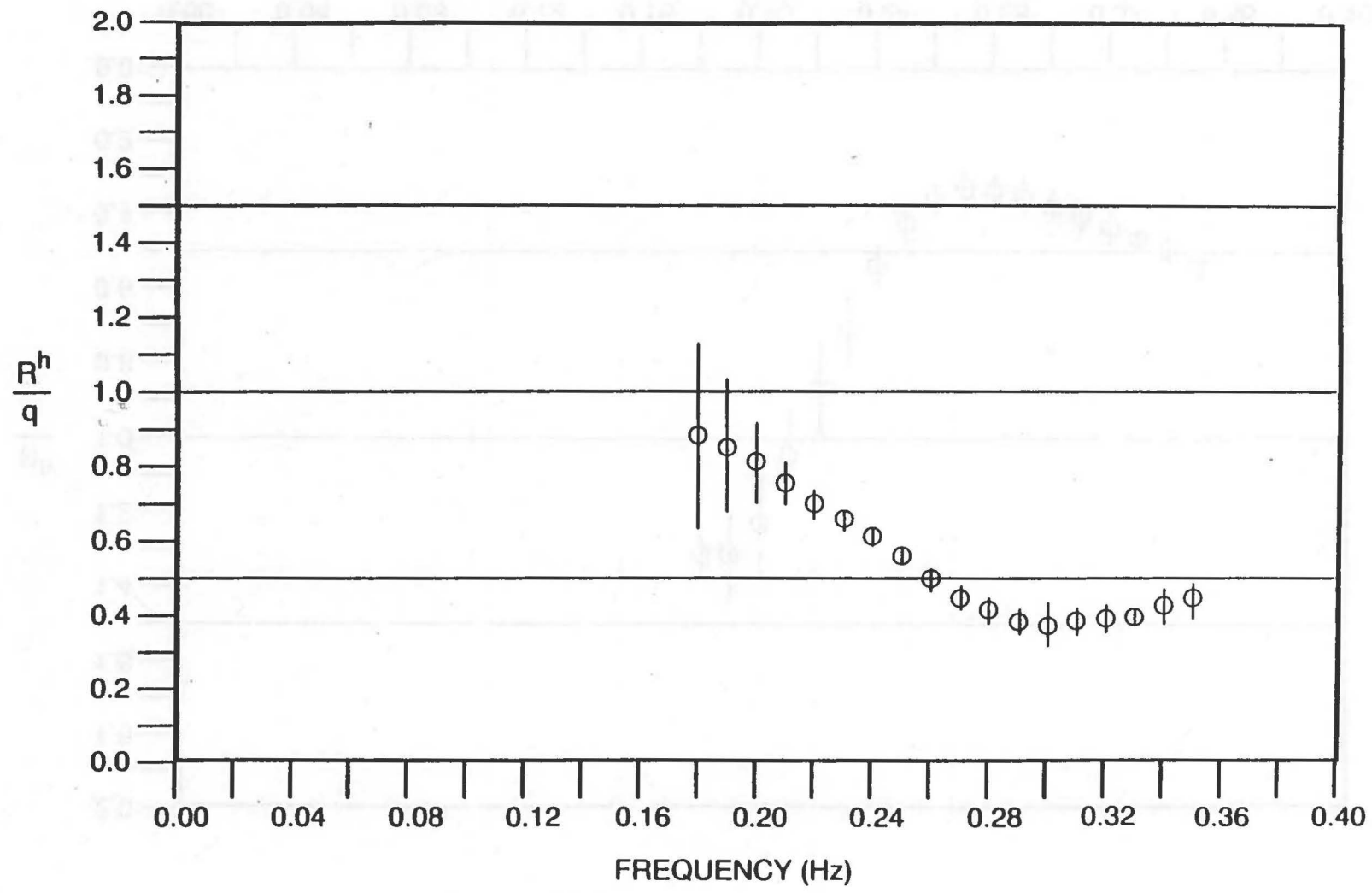


Figure 12. Means and Standard Deviations of R^h/q Versus Frequency, for Wind Speeds In Range $(10 \leq U \text{ (M/Sec)} < 12)$, Limited Data Set

not consistently overlap, R^h/q appears to vary with wind speed, possibly because of changes in mooring line tension.

These changes could also alter ϕ^h , the angle associated with R^h/q . This possibility was investigated and the results appear in Figures 13 and 14. Once again, there are apparent changes in ϕ^h as the wind increases. It is these variations in $(R^h/q, \phi^h)$ that necessitate the use of equations (6), (8), and (9) each hour to adjust for variations in the effect of wind speed on hull-mooring response.

7.0 CONCLUDING REMARKS

The bridle below the buoy, which provides excellent stability in severe winds and waves, does not prevent the hull from following the slope of the sea surface well enough to allow directional wave measurements. The parameters $(R^h/q, \phi^h)$ vary somewhat from station to station due to mooring design differences, and for a particular buoy in response to wind speed. However, these functions can be regarded as constants during the 20 minutes of wave data acquisition, and can be determined from the measurements taken during that 20 minutes.

There are several design features of the 3-meter DACT DWA that need improvement. All drag asymmetries in the superstructure need to be removed. If the buoy is to provide high quality data in hurricane force winds, the superstructure needs minor redesign to lower the drag force somewhat. And if operating costs are to be lowered further, the longevity of the power system must be extended from the present 15 to 18 months to 2 years, or to 3 years if possible. Efforts are now under way at NDBC to make these improvements.

8.0 ACKNOWLEDGEMENTS

Many others are due credit for the basic 3-meter buoy, its payload, and its meteorological measurements system. Furthermore, several persons other than the authors have contributed to the success of the 3-meter DACT DWA wave measurements. Mr. Doug Scally of NDBC designed the buoy center-compartment-rack containing the power, sensor, and electronics subsystems. Ms. K. Tullock of Magnavox Corporation implemented the software used in the DWA. Early on Mr. Joe Lau, and later on Mr. Frank Remond, of Computer Sciences Corporation, and Mr. William Owens of Sverdrup Corporation, all contributed significantly to the refinement of system testing procedures. Ms. Charlene Stephens of CSC designed the graphics programs that are specific to DWA directional wave data. Mr. Lloyd Ladner, Program Manager for the NDBC Moored Buoy Program, has directed the integration and field operations for all operational 3-meter DACT DWA buoys, including the one deployed at station 45005.

9.0 REFERENCES

- [1] M. S. Longuet-Higgins, D. E. Cartwright, and N. D. Smith, "Observations of the Directional Spectrum of Sea Waves Using the Motions of a Floating Buoy," in OCEAN WAVE SPECTRA. Englewood Cliffs, NJ: Prentice-Hall, 1963.
- [2] S. Barstow and J. Guddal, "A Global Survey on the Need for and Application of Directional Wave Information," World Meteorological Organization, Marine Meteorology and Related Oceanographic Activities Report No. 19, WMO/TD - No. 209, 1987.

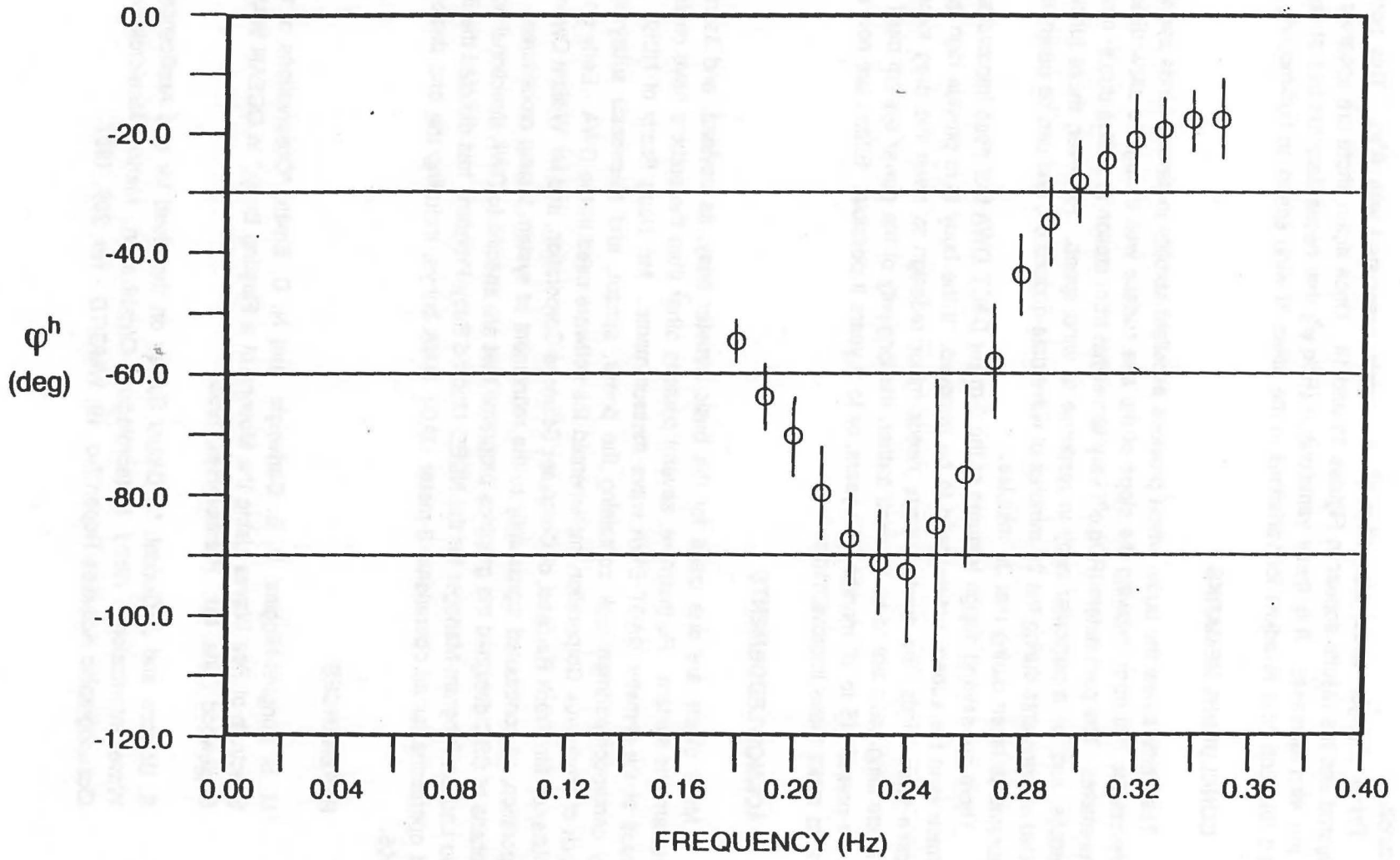


Figure 13. Means and Standard Deviations of ϕ^h Versus Frequency, for $(4 \leq U \text{ (M/Sec)} < 5)$, Limited Data Set

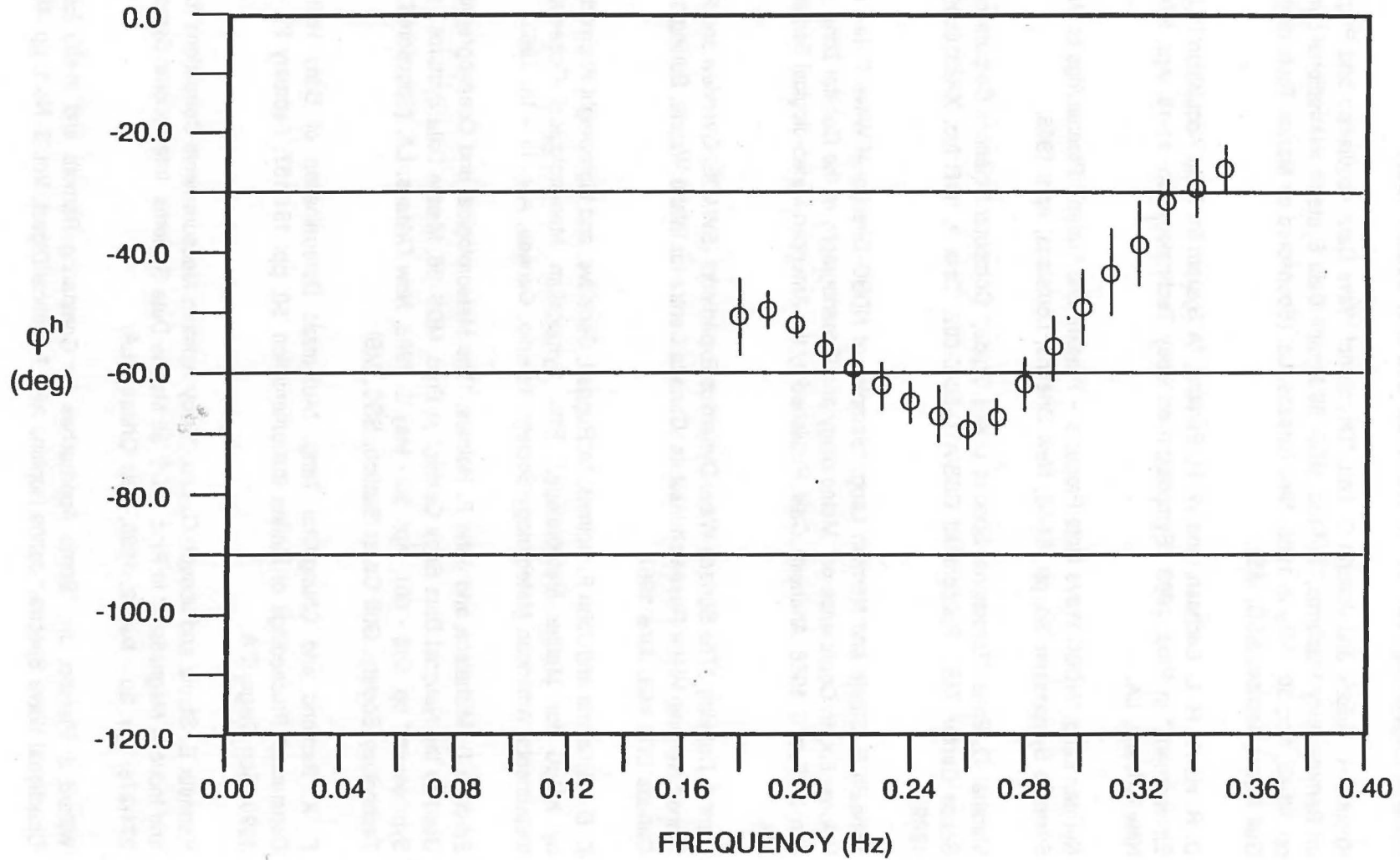


Figure 14. Means and Standard Deviations of ϕ^h Versus Frequency for $(10 \leq U \text{ (M/Sec)} < 12)$, Limited Data Set

- [3] Kenneth E. Steele, Joseph Chi-Kin Lau, and Yuan-Huang L. Hsu, "Theory and Application of Calibration Techniques for an NDBC Directional Wave Measurements Buoy," IEEE Journal of Oceanic Engineering, Vol. OE-10, No. 4, pp. 382-396, October 1985.
- [4] Kristina H. Tullock and Joseph C. Lau, "Directional Wave Data Acquisition and Preprocessing on Remote Buoy Platforms," in Proc. MDS '86 Marine Data Systems International Symposium," pp. 43-48, Apr. 30 - May 2, 1986, New Orleans, La. (Sponsored by Marine Technology Society, Gulf Coast Section, SSC, MS).
- [5] D. R. Howe, R. L. Erichsen, and W. H. Serstad, "A System for Data Acquisition in the Ocean Environment," in Proc. 1983 Symposium on Buoy Technology, pp. 11-18, Apr. 27-29, 1983, New Orleans, LA.
- [6] Norman Lang, "NDBC Wave Data Products -- Present and Future," Proceedings of Marine Data Systems Symposium '86, pp. 54-58, New Orleans, Louisiana, April 1986.
- [7] Marshall D. Earle, "Directional Spectra User's Guide," Computer Sciences Corporation, Stennis Space Center, MS. Subcontract CSS/ATD-88-C-002, Task 9, IWR No. XA2310809, January 1989.
- [8] Kenneth E. Steele and Norman Lang, "Samples of NDBC Directional Wave Data," in Preprint Volume Fourth Conference on Meteorology and Oceanography of the Coastal Zone, pp. 50-57, Jan. 31-Feb. 5, 1988, Anaheim, Calif. Published by the American Meteorological Society, Boston, MA.
- [9] Mark A. Donelan, "The Surface Wave Dynamics Experiment (SWADE) Overview and Preliminary Plans," National Water Research Institute, Canada Centre for Inland Waters, Burlington, Ontario, Canada L7R 4A6, June 1987.
- [10] E. D. Michelena and John F. Holmes, "A Rugged, Sensitive, and Lightweight Anemometer Used by NDBC for Marine Meteorology," Fifth Symposium Meteorological Observations and Instruments, American Meteorology Society, Toronto, Canada, Apr. 11 - 15, 1983.
- [11] Eduardo D. Michelena and John F. Holmes, "The Meteorological and Oceanographic Sensors Used by the National Data Buoy Center," in Proc. MDS '86, Marine Data Systems International Symposium," pp. 596 - 601, Apr. 30 - May 2, 1986, New Orleans, LA. (Sponsored by Marine Technology Society, Gulf Coast Section, SSC, MS).
- [12] F. X. Remond and Chung-Chu Teng, "Automatic Determination of Buoy Hull Magnetic Constants," Proceedings of Marine Instrumentation '90, pp. 151-157, February 27 - March 1, 1990, San Diego, CA.
- [13] Kenneth E. Steele and Joseph C. Lau, "Buoy Azimuth Measurements-Corrections for Residual and Induced Magnetism," in Proc. MDS '86 Marine Data Systems International Symposium, pp. 271-276, Apr. 30 - May 2, 1986, New Orleans, LA.
- [14] Willard J. Pierson, Jr., "Some Approaches for Comparing Remote and in-situ Estimates of Directional Wave Spectra," Johns Hopkins APL Technical Digest, Vol. 8, No.1, pp. 48-54, 1987.

- [15] K. E. Steele, J. Michael Hall, and F. X. Remond, "Routine Measurement of Heave Displacement Spectra from Large Discus Buoys in the Deep Ocean," in Proc. 1st Combined IEEE Conf. OCEAN 75 (San Diego, CA), pp. 79-87, Sept. 1975.
- [16] J. Lee, "A Study of Hull-Mooring Data Bases for Wave Measurement Systems," Computer Sciences Corporation, National Data Buoy Center, SSC, MS, Nov. 1984 (NDBC internal document).
- [17] W. D. Kim, "On the Forced Oscillations of Shallow-draft Ships," *Journal of Ship Research*, Vol. 7, No. 2, October 1963.
- [18] Robert H. Stewart, "A Discus-hulled Wave Measuring Buoy," *Ocean Engng.*, Vol. 4, pp. 101-107, Pergamon Press, 1977, printed in Great Britain.
- [19] D. E. Barrick, B. J. Lipa, and Kenneth E. Steele, "Comments on Theory and Application of Calibration Techniques for an NDBC Directional Wave Measurements Buoy: Nonlinear Effects," *IEEE Journal of Oceanic Engineering*, Vol. 14, No. 3, pp. 268, July 1989.
- [20] N. C. Lang, "A Study of Noise and Transfer Properties for Slope Spectra as Measured by a Pitch/Roll Buoy," Computer Sciences Corporation, National Data Buoy Center, SSC, MS, July 1988 (NDBC in-house document).
- [21] Larry Hsu, "Evaluation of E-buoy and Other Wave Data," U. S. Department of Commerce NOAA Report F-344-6, September 1984.
- [22] Users manual for the National Data Buoy Center COMPAQ Directional Wave Simulator, Sverdrup Technology Corporation Scientific Technology Corporation, SSC, MS, January 1988.
- [23] Norman C. Lang, "An Algorithm for the Quality Checking of Wind Speeds Measured at Sea Against Measured Wave Spectral Energy," *IEEE Journal of Oceanic Engineering*, Vol. OE-12, No. 4, pp. 560-567, October 1987.
- [24] David B. Gilhousen, "NDBC Directional Wave Measurements," *Proceedings of Instrumentation '90*, pp. 110-117, February 27 - March 1, 1990, San Diego, CA.
- [25] David Wei-Chi Wang, Chung-Chu Teng, and Kenneth E. Steele, "Buoy Directional Wave Observations in High Seas," *Proceedings of OCEANS '89*, pp. 1416-1420, Seattle, Washington, October 1989.
- [26] Kenneth E. Steele, "Directional Wave Data from Lake Erie," *National Data Buoy Center Technical Bulletin*, Vol. 16, No. 1, January 1990.
- [27] David Wei-Chi Wang, "Estimating Wind Direction from a Small Discus Buoy," *Proceedings of Marine Instrumentation '90*, pp. 168-177, February 27 - March 1, 1990, San Diego, CA.

101. The first part of the document is a list of names and addresses of the members of the committee. The names are listed in alphabetical order and include the following: [illegible names]

102. The second part of the document is a list of the names and addresses of the members of the committee who have resigned. The names are listed in alphabetical order and include the following: [illegible names]

103. The third part of the document is a list of the names and addresses of the members of the committee who have been elected. The names are listed in alphabetical order and include the following: [illegible names]

104. The fourth part of the document is a list of the names and addresses of the members of the committee who have been re-elected. The names are listed in alphabetical order and include the following: [illegible names]

105. The fifth part of the document is a list of the names and addresses of the members of the committee who have been appointed. The names are listed in alphabetical order and include the following: [illegible names]

106. The sixth part of the document is a list of the names and addresses of the members of the committee who have been elected to the office of [illegible office]. The names are listed in alphabetical order and include the following: [illegible names]

107. The seventh part of the document is a list of the names and addresses of the members of the committee who have been elected to the office of [illegible office]. The names are listed in alphabetical order and include the following: [illegible names]

108. The eighth part of the document is a list of the names and addresses of the members of the committee who have been elected to the office of [illegible office]. The names are listed in alphabetical order and include the following: [illegible names]

109. The ninth part of the document is a list of the names and addresses of the members of the committee who have been elected to the office of [illegible office]. The names are listed in alphabetical order and include the following: [illegible names]

110. The tenth part of the document is a list of the names and addresses of the members of the committee who have been elected to the office of [illegible office]. The names are listed in alphabetical order and include the following: [illegible names]

APPENDIX A. DISSEMINATION OF ENVIRONMENTAL DATA

A.1 NWSTG DATA PROCESSING AND DISTRIBUTION

The original hourly data from a 3-meter DACT DWA buoy are relayed through GOES to the Command and Data Acquisition facility of the National Environmental Satellite, Data, and Information Service. Here the data are monitored and forwarded to the National Weather Service Telecommunications Gateway (NWSTG). At the NWSTG these data are processed and disseminated to operational users. Meteorological data are also sent to the National Meteorological Center for use in meteorological models, which provide forecast data to NWSTG for distribution to users. The original buoy data and all processed data are forwarded to NDBC for detailed quality control and system analysis.

The wave data processing and dissemination at NWSTG are documented in references [6] and [7]. Values of C_{11} , r_1 , α_1 , r_2 , and α_2 (see Section 2.0) are calculated and used to determine $S(f,\alpha)$ with equations (1) and (2). $S(f,\alpha)$ is computed for each 0.01-Hz band at 2-degree steps around the azimuth circle, and the angle (peak wave direction) associated with the largest energy value is determined. The 0.01-Hz bands listed in Table A1 are used to define 15 bands with varying widths, some containing several 0.01-Hz bands. For each of these 15 bands, the 0.01-Hz band containing the most energy is located, and its peak wave direction is attached to the broad band within which it lies. The spectral energy and peak wave direction for each of these 15 bands is transmitted in real time each hour from NWSTG to National Weather Service Forecast Offices through an AFOS (Automation of Field Operations and Services) message [7]. The message length limitations of the AFOS system not only necessitate a loss of spectral detail through the averaging of 0.01-Hz bands, but reports are also transmitted only every third hour.

Table A1. AFOS Wave Spectrum Bands

BAND NUMBER	CENTER FREQUENCY (Hz)	BAND WIDTH (Hz)
1	0.31	0.09
2	0.24	0.05
3	0.195	0.04
4	0.16	0.03
5	0.135	0.02
6	0.12	0.01
7	0.11	0.01
8	0.10	0.01
9	0.09	0.01
10	0.08	0.01
11	0.07	0.01
12	0.06	0.01
13	0.05	0.01
14	0.04	0.01
15	0.03	0.01

A.2 NDBC DATA PROCESSING AND DISTRIBUTION

The original and processed buoy data are sent by the NWSTG to NDBC at SSC. At SSC, the data processed at NWSTG are compared to the corresponding data processed at NDBC, to ensure quality. Quality controlled records of C_{11} , r_1 , α_1 , r_2 , α_2 , and C_{11}^S (see Section V) produced at NDBC, together with corresponding meteorological data, are routinely archived at the National Oceanographic Data Center (NODC) and the National Climatic Data Center (NCDC) within 30 days. NODC (202-673-5549) and NCDC (704-259-0682) are the authorized U.S. government sources for these data. Significant wave height, average wave period, and peak wave period are the only wave data available from NCDC. All wave data are available from NODC.

A.3 INTERNATIONAL DISTRIBUTION

Recently the World Meteorological Organization approved a new code (WAVEOB) for the distribution of directional wave data on international circuits. Data in this format will also be disseminated on the NWS Family of Services, and will be available to on-line data bases maintained by private meteorological firms.

STATION	TYPE	STATUS
100	1	1
101	1	1
102	1	1
103	1	1
104	1	1
105	1	1
106	1	1
107	1	1
108	1	1
109	1	1
110	1	1
111	1	1
112	1	1
113	1	1
114	1	1
115	1	1
116	1	1
117	1	1
118	1	1
119	1	1
120	1	1

APPENDIX B. BUOY CONFIGURATION

B.1 HULL AND MOORINGS

The 3-meter-diameter hull is shown in Figure 1. This design results from significant modifications made by NDBC in 1982-3 to a design obtained from the Woods Hole Oceanographic Institution (WHOI). The modified hull is fabricated from an aluminum alloy and has six void compartments surrounding a central 0.9144-meter-diameter by 1.016-meter-deep ventilated equipment compartment. A three-legged aluminum-alloy mast, which folds to permit crane access to the central compartment, is bolted to pads on the hull deck. The buoy at station 45005 had a fin of the smaller size as indicated in Figure 1. All NDBC 3-meter directional buoys now make use of the larger fin, shown in outline.

Solar panels, a marker light, radar reflectors, antennas, and meteorological sensors are mounted on the mast. Identical anemometers are mounted at positions 3.7 and 4.9 meters above the hull design waterline. Two air temperature sensors are mounted at 3.5 meters above this line. Two barometric pressure sensors located at the waterline, a heave-pitch-roll sensor, a triaxial magnetometer used for wave measurements, the DACT DWA electronics, a compass used for wind direction measurements, and the primary and secondary battery systems are installed on a removable aluminum rack in the center cylindrical compartment. Fully integrated, the hull displaces approximately 1500 kg with 2700 kg additional reserve buoyancy.

The three-legged steel bridle below the hull attaches to a 25-foot chain. This chain connects through a swivel to the remainder of the mooring, the design of which depends on station-specific factors. The bridle provides good hydrostatic stability at an acceptable loss of the wave-slope-following response necessary to make directional wave measurements. All-chain and inverse-catenary are the two types of moorings thus far used with the 3-meter DACT DWA buoy. The mooring design for a particular station depends on water depth, sea bottom conditions, salinity, and duration of deployment.

B.2 POWER SYSTEM

To be cost-effective, the buoy must be designed to collect meteorological and ocean data over a period of years. Operating costs depend significantly on the interval between visits to the site, so longevity for the power system is needed. The 3-meter DACT DWA power system includes primary batteries, secondary batteries, solar panels, 115-volt AC power, and a Power Control Unit. Solar panels charge the secondary batteries, from which power is drawn when solar energy is not directly available or is not completely adequate. Power from the primary batteries is used only when inadequate power is available from the solar panels and secondary batteries. Of course, the lifetime of this system depends on the solar energy available at the deployment station.

Significant energy from the primary batteries is used in testing the system prior to deployment. A 115 VAC power source is used during dockside testing to reduce this energy loss. On station, a buoy typically operates 15 to 18 months, reporting data hourly, before the primary batteries are depleted and the buoy must be retrieved.

B.3 COMMUNICATION SYSTEMS

The meteorological and wave data are formatted and transmitted hourly via a GOES message that fits into a 2-minute window. Within this window, the first and last 15 seconds are not used so that DACT clock drift will not be likely to cause interference with other buoys reporting in adjacent windows. The first 8 seconds of the 90-second message set up the buoy-satellite connection. With

the GOES transmission rate of 100 bits/sec and the required ASCII code control and parity bits, a total of 6150 data bits are relayed in the remaining 82 seconds. Of these, 700 comprise meteorological data, and 5450 directional (including non-directional) wave data. The block of wave data consists of 334 11-bit words, the first 59 containing system monitoring and nondirectional wave data. Remaining words contain directional information.

The position of the buoy at 45005 is determined by LORAN-C and is transmitted hourly through GOES. Other position fixing techniques (e.g., Argos, Local-User-Terminal) are sometimes used with 3-meter DACT DWA buoys. A mooring failure, should it occur, is usually detected within hours as a buoy drifts outside its "watch" circle.

Ideally, meteorological and wave data from all buoys in the NDBC network would be acquired simultaneously and reported to shore simultaneously. But since each buoy has its own reporting-time window in one of only two GOES channels available to NDBC, and these time windows are not in all cases located at convenient times during the hour, this ideal cannot be achieved; DACT DWA meteorological and wave data are acquired at different times on the same buoy, and transmitted to GOES at different times on different buoys. Thus, unless environmentally stationary conditions exist, data users should be cautious in relating to each other meteorological and wave data from the same station and attached to the same hour, and in relating either of these data sets to other sources of data attached to the same hour for a particular station.

For example, the 3-meter DACT DWA buoy at station 45005 started the 20-minute wave data acquisition period at 25 minutes after the hour. Meteorological measurements began at 44 minutes after the hour, when wave data acquisition ended. Both data sets were reported through GOES beginning at 57 minutes after the hour, and at shore the data were time-tagged with the next hour. NDBC can provide to users details of acquisition and reporting times for any particular buoy.

B.4 METEOROLOGICAL MEASUREMENT SYSTEMS

Table B1 summarizes the meteorological data produced by the DACT. Wind speed and direction based on 8-minute averages, and wind speed gust based on 8-second averages, are produced from two R. M. Young Wind Monitor anemometers [10] and a Digicourse model 101 compass [11], mounted as described in Appendix A.

Air temperature is measured by two Yellow Springs P/N thermistors. Two thermistors of this same type, each with a linearizing circuit and sealed in epoxy in a copper slug clamped to the inside to the hull and covered by an insulating plastic housing, are used for the measurement of water temperature [11]. Two Rosemont model 1201F2 transducers located inside the payload compartment at the waterline are used to measure sea-level pressure.

The outputs of all meteorological sensors are connected to the DACT payload, which samples these outputs each hour and transmits processed data through GOES to shore. The DACT also manages the directional wave data produced by the DWA system, as described in Section 2.0.

Table B1. Overall Measurement Characteristics of the Meteorological Variables Reported by the DACT Payload

Parameter	Reporting Range	Reporting Resolution	Sample Interval	Sample Period	Total System Accuracy
Wind Speed	0 to 80 m/s	0.1 m/s	1 sec	8.0 min	± 1 m/s or 10%
Wind Direction	0 to 360°	1°	1 sec	8.0 min	± 10°
Wind Gust*	0 to 80 m/s	0.1 m/s	1 sec	8.0 min	± 1 m/s or 10%
Air Temperature	-40° to 50°C	0.5°C	90 sec	90 sec	± 1°C
Barometric Pressure	900 to 1100 hPa (mb)	0.1 hPa (mb)	4 sec	8.0 min	± 1 hPa (mb)
Surface Water Temp.	-15° to 50°C	0.5°C	1 sec	1 sec	± 1°C

*Highest 8-second window average retained

TABLE 2.1. Summary of the 1990-1991
 Annual Report of the Board of Directors

Category	1990-1991	1989-1990	1988-1989	1987-1988	1986-1987
Operating Income	1,200,000	1,100,000	1,000,000	900,000	800,000
Net Income	800,000	750,000	700,000	650,000	600,000
Dividends Paid	400,000	350,000	300,000	250,000	200,000
Retained Earnings	400,000	400,000	400,000	400,000	400,000
Total Assets	10,000,000	9,500,000	9,000,000	8,500,000	8,000,000
Total Liabilities	4,000,000	3,800,000	3,600,000	3,400,000	3,200,000
Total Equity	6,000,000	5,700,000	5,400,000	5,100,000	4,800,000

* Figures are in thousands of dollars.

APPENDIX C. PREDEPLOYMENT TESTING AND CALIBRATION

For validation and calibration purposes, the 3-meter DACT DWA end-to-end system is divided into three subsystems:

- (a) Hull and mooring
- (b) Sensors
- (c) Onboard electronics with its data processing and data transmission systems, and shoreside data processing and distribution systems

Since data processing does not consider ocean currents and assumes linear small amplitude wave theory, the DWA system is "self-calibrating" so far as the effects of the hull-mooring on (r_1 , α_1 , r_2 , α_2) are concerned. There are no predetermined table calibrations relating to (a) except for the ϕ table and the dependency of C_{11} on R^{hh} through PTF. No field testing of any particular 3-meter DWA hull-mooring is done to establish R^{hh} for that combination. R^{hh} values from a field calibration [21] of a 3-meter hull-mooring against a Datowell Waverider are used for all 3-meter buoys, taking account of water depth. On the basis of this calibration, unity is used for R^{hh} values at station 45005 in the bands [0.03(0.01)0.35] Hz. Since simulation models indicate that the R^{hh} function is insensitive to the details of the mooring design, ignoring variations in mooring designs from station to station is probably technically sound as well as unavoidable when many buoys are deployed. R^{hh} values are estimated to be accurate to ± 5 percent.

With regard to (b), Datowell RAO data for the HIPPY 40 Mark II heave displacement voltages are verified to be within bounds with the Ocean Wave Instrumentation Facility (OWIF) before installation in the buoy. The OWIF, located at NDBC at SSC, is a "ferris-wheel" type system of radius 1-2 meters. In addition, pitch and roll are verified for the completed buoy configuration in still water at dockside by tilting the hull deck with suspended weights. Pitch and roll sensor output voltages, and the associated 20-minute values of minimum, mean, and maximum reported to shore, are verified to be within expected ranges. Magnetometers are qualified by laboratory tests before installation in the hull.

For the third subsystem (c), parts are not only complex, but located at several different government installations. Controlled voltages simulating the sensor outputs for eight hull-azimuth angle and single-frequency-wave combinations are generated by a "sensor simulator," and input to the DACT DWA. Then the final output wave data are verified at each of these installations; except for sensor voltages being simulated, these are end-to-end tests. This sensor simulator [22] comprises a computer that generates digital time series of sensor outputs, and a digital-to-analog converter that translates these into voltages for input to the DACT DWA.